

# Current and potential imaging applications of ferumoxytol for magnetic resonance imaging

Gerda B. Toth<sup>1,21</sup>, Csanad G. Varallyay<sup>2,21</sup>, Andrea Horvath<sup>1,21</sup>, Mustafa R. Bashir<sup>3,4</sup>, Peter L. Choyke<sup>5</sup>, Heike E. Daldrup-Link<sup>6</sup>, Edit Dosa<sup>7</sup>, John Paul Finn<sup>8</sup>, Seymour Gahramanov<sup>9</sup>, Mukesh Harisinghani<sup>10</sup>, Iain Macdougall<sup>11</sup>, Alexander Neuwelt<sup>12</sup>, Shreyas S. Vasanawala<sup>13</sup>, Prakash Ambady<sup>1</sup>, Ramon Barajas<sup>2</sup>, Justin S. Cetas<sup>14</sup>, Jeremy Ciporen<sup>14</sup>, Thomas J. DeLoughery<sup>15</sup>, Nancy D. Doolittle<sup>1</sup>, Rongwei Fu<sup>16,17</sup>, John Grinstead<sup>18</sup>, Alexander R. Guimaraes<sup>2</sup>, Bronwyn E. Hamilton<sup>2</sup>, Xin Li<sup>19</sup>, Heather L. McConnell<sup>1</sup>, Leslie L. Muldoon<sup>1</sup>, Gary Nesbit<sup>2</sup>, Joao P. Netto<sup>1,2</sup>, David Petterson<sup>2</sup>, William D. Rooney<sup>19</sup>, Daniel Schwartz<sup>1,19</sup>, Laszlo Szidonya<sup>1</sup> and Edward A. Neuwelt<sup>1,14,20</sup>

<sup>1</sup>Department of Neurology, Oregon Health & Science University, Portland, Oregon, USA; <sup>2</sup>Department of Radiology, Oregon Health & Science University, Portland, Oregon, USA; <sup>3</sup>Department of Radiology, Duke University Medical Center, 3808, Durham, North Carolina, USA; <sup>4</sup>Center for Advanced Magnetic Resonance Development, Duke University Medical Center, Durham, North Carolina, USA; <sup>5</sup>Molecular Imaging Program, Center for Cancer Research, National Cancer Institute, National Institutes of Health, Bethesda, Maryland, USA; <sup>6</sup>Department of Radiology, Section of Pediatric Radiology, Lucile Packard Children's Hospital, Stanford University, 725 Welch Rd, Stanford, California, USA; <sup>7</sup>Heart and Vascular Center, Semmelweis University, Budapest, Hungary; <sup>8</sup>Department of Radiological Sciences, David Geffen School of Medicine, University of California, Los Angeles, California, USA; <sup>9</sup>Department of Neurosurgery, University of New Mexico Health Sciences Center, Albuquerque, New Mexico, USA; <sup>10</sup>Department of Radiology, Harvard Medical School, Massachusetts General Hospital, Boston, Massachusetts, USA; <sup>11</sup>Department of Renal Medicine, King's College Hospital, London, UK; <sup>12</sup>Division of Medical Oncology, University of Colorado Denver, Aurora, Colorado, USA; <sup>13</sup>Department of Radiology, Stanford University, Stanford, California, USA; <sup>14</sup>Department of Neurosurgery, Oregon Health & Science University, Portland, Oregon, USA; <sup>15</sup>Department of Hematology and Medical Oncology, Oregon Health & Science University, Portland, Oregon, USA; <sup>16</sup>School of Public Health, Oregon Health & Science University, Portland, Oregon, USA; <sup>17</sup>Department of Medical Informatics and Clinical Epidemiology, Oregon Health & Science University, Portland, Oregon, USA; <sup>18</sup>Siemens AG, Healthcare Center, Portland, Oregon, USA; <sup>19</sup>Advanced Imaging Research Center, Oregon Health & Science University, Portland, Oregon, USA; and <sup>20</sup>Portland Veterans Affairs Medical Center, Portland, Oregon, USA

Contrast-enhanced magnetic resonance imaging is a commonly used diagnostic tool. Compared with standard gadolinium-based contrast agents, ferumoxytol (Feraheme, AMAG Pharmaceuticals, Waltham, MA), used as an alternative contrast medium, is feasible in patients with impaired renal function. Other attractive imaging features of i.v. ferumoxytol include a prolonged blood pool phase and delayed intracellular uptake. With its unique pharmacologic, metabolic, and imaging properties, ferumoxytol may play a crucial role in future magnetic resonance imaging of the central nervous system, various organs outside the central nervous system, and the cardiovascular system. Preclinical and clinical studies have demonstrated the overall safety and effectiveness of this novel contrast agent, with rarely occurring anaphylactoid reactions. The purpose of this review is to describe the general and organ-specific properties of ferumoxytol, as well as the advantages and potential pitfalls associated with its use in magnetic resonance imaging. To more fully demonstrate the applications of ferumoxytol throughout

the body, an imaging atlas was created and is available online as supplementary material.

*Kidney International* (2017) ■, ■-■; <http://dx.doi.org/10.1016/j.kint.2016.12.037>

KEYWORDS: chronic kidney disease; magnetic resonance imaging; nephrotoxicity

Published by Elsevier, Inc., on behalf of the International Society of Nephrology.

## PURPOSE OF THIS REVIEW

Since the US Food and Drug Administration (FDA) approved ferumoxytol (Feraheme, AMAG Pharmaceuticals, Waltham, MA, USA) to treat iron deficiency anemia in adults with chronic kidney disease (CKD) in 2009, the off-label use of this iron oxide nanoparticle compound by clinicians and researchers as a magnetic resonance imaging (MRI) contrast agent has rapidly grown. Ferumoxytol-enhanced imaging is feasible in patients with impaired renal function, a patient population in whom both gadolinium and iodinated contrast agents are contraindicated. Other attractive imaging features of i.v. ferumoxytol include a prolonged blood pool phase and delayed intracellular uptake. Furthermore, because iron is a naturally occurring element in the body, the administered iron enters the body's natural iron metabolic pathways. Thus, the use of ferumoxytol is not currently associated with concerns regarding long-term deposition, as is the case with brain deposition of gadolinium-containing agents.<sup>1-4</sup>

**Correspondence:** Edward A. Neuwelt, Blood-Brain Barrier Program, Oregon Health & Science University, Portland, OR 97239. E-mail: [neuwalte@ohsu.edu](mailto:neuwalte@ohsu.edu)

<sup>21</sup>These authors contributed equally to this manuscript.

Received 15 September 2016; revised 17 November 2016; accepted 6 December 2016

There are 2 aims of this review: first, to draw attention to a viable option of contrast-enhanced cross-sectional imaging in patients with renal failure; therefore, *Kidney International* was chosen for publication, and second, to highlight the growing body of literature that explores a variety of clinical indications that suggest ferumoxytol has utility not only as an alternative to gadolinium-based contrast agents (GBCAs) but also as a specialized MRI contrast agent with unique properties.

The number of clinical trials that use ferumoxytol as a contrast agent is increasing. The coauthors are experienced in the imaging of the central nervous system (CNS), body, and cardiovascular system with ferumoxytol. Based on the recommendations of the coauthors, we collected relevant articles in the literature focusing on ferumoxytol over other ultrasmall superparamagnetic iron oxides (USPIOs) and highlighted the clinical applications rather than the preclinical investigations.

This article describes ferumoxytol administration, dosing, and timing for imaging applications, followed by organ-specific utilizations. We created an atlas ([Supplementary Material 1](#)) that more fully describes the application of ferumoxytol throughout the body and a table of relevant clinical publications ([Supplementary Material 2](#)) that use ferumoxytol, both of which can be found in the [online supplement](#).

### FERUMOXYTOL AS AN IRON REPLACEMENT

I.v. iron supplementation is important in patients with CKD owing to poor gastric absorption of oral iron. Insufficient absorption is related to the upregulation of hepcidin that occurs in CKD,<sup>5</sup> which is exacerbated by excessive iron losses.

Although widely used, iron dextran, iron sucrose, and iron sodium gluconate have significant clinical limitations. Over the last decade, 3 new i.v. iron preparations have been developed that display tighter iron binding, allowing greater doses of iron to be given in a single administration. Along with ferric carboxymaltose and iron isomaltoside 1000, ferumoxytol has entered the therapeutic arena as an effective iron supplement.<sup>5</sup> Ferumoxytol has favorable physicochemical characteristics, potentially reducing amounts of circulating free iron.<sup>6</sup> Multiple studies have reported effective and safe treatments of iron deficiency with ferumoxytol.<sup>7–9</sup>

### FERUMOXYTOL IN MRI

Initially, ferumoxytol was developed as an MRI contrast agent because of its effectiveness in shortening T1 and T2 relaxation times. Licensing the drug as a therapeutic iron supplement was likely a strategic decision, but this compound still holds great potential as an MRI contrast agent. Satisfactory contrast-enhanced imaging can be performed with doses as low as 1 mg/kg and as high as a 510 mg total dose. See [Figure 1](#) for the potential imaging phases following i.v. administration.

Arterial-venous dynamic phase: T2\*-based dynamic susceptibility contrast perfusion imaging of the brain requires only 1 mg/kg ferumoxytol and provides parametric maps of the brain similar to those achieved with a standard dose of gadolinium.<sup>10</sup> The lack of early contrast extravasation with ferumoxytol is beneficial in cardiovascular and peripheral

vascular examinations, wherein T1-weighted images acquired using a 4-mg/kg bolus injection clearly show intravascular enhancement as hyperintense structures. Although there is no evidence that these small bolus injections carry a higher risk of adverse events, rapid injection of ferumoxytol is not currently recommended by the FDA.<sup>11</sup>

Blood pool phase: One of the major advantages of nanoparticle imaging is the relatively long circulating time, with ferumoxytol displaying a plasma half-life of 14 to 21 hours. Even in highly permeable tumors, high-resolution imaging of the intravascular space can be achieved without visible background tissue enhancement. Steady-state blood volume mapping of the brain is a T2\*-based technique that requires 3 to 7 mg/kg ferumoxytol,<sup>12,13</sup> whereas T1-based steady-state angiography of the peripheral vessels is performed using 3 to 4 mg/kg.<sup>14</sup>

Delayed phase: In brain lesions, slow leakage of ferumoxytol through the disrupted blood-brain barrier results in MRI signal changes peaking around 24 hours after ferumoxytol administration.<sup>15</sup> T1-weighted MRI shows signal increases similar to those observed with gadolinium. A signal decrease on T2/T2\*-weighted images may represent high local iron concentration and/or intracellular uptake, which has many useful applications outside of the CNS. Indeed, the intracellular uptake of ferumoxytol in abdominal organs, lymph nodes, and vascular walls can be used to effectively delineate pathology in these areas.<sup>16,17</sup>

It is important to note that if a subsequent MRI is needed within 72 hours, ferumoxytol contrast enhancement may still be present in brain pathologies several days following administration.<sup>15</sup> In addition, decreased signal intensities in the liver, spleen, and bone marrow scans may persist for several months before returning to baseline.

### FERUMOXYTOL METABOLISM AND CLEARANCE

Following extravasation, ferumoxytol nanoparticles are taken up by cells of the mononuclear phagocyte system (MPS, previously known as the reticuloendothelial system), primarily in the liver, spleen, and bone marrow. In the brain, macrophages or astrocytes contribute to ferumoxytol clearance.<sup>18,19</sup> Within these phagocytic cells, the nanoparticles are stored in secondary lysosomes ([Figure 2](#)).<sup>19</sup> The carboxymethyl-dextran coating is cleaved by dextranase and the cleaved coating is completely excreted by the kidneys and/or eliminated through feces. The iron core is incorporated into the body's iron stores and used for cell metabolism and hemoglobin synthesis. Unless the patient has known hemosiderosis or hemochromatosis, the administered iron during MRI examination (maximum, 510 mg) is safe, and no overloading occurs.<sup>20</sup>

[Table 1](#) summarizes the physical, pharmacokinetic, and imaging properties of ferumoxytol compared with those of gadolinium.

### FERUMOXYTOL SAFETY

On March 30, 2015, the FDA revised the prescribing information of Feraheme to include the addition of a boxed

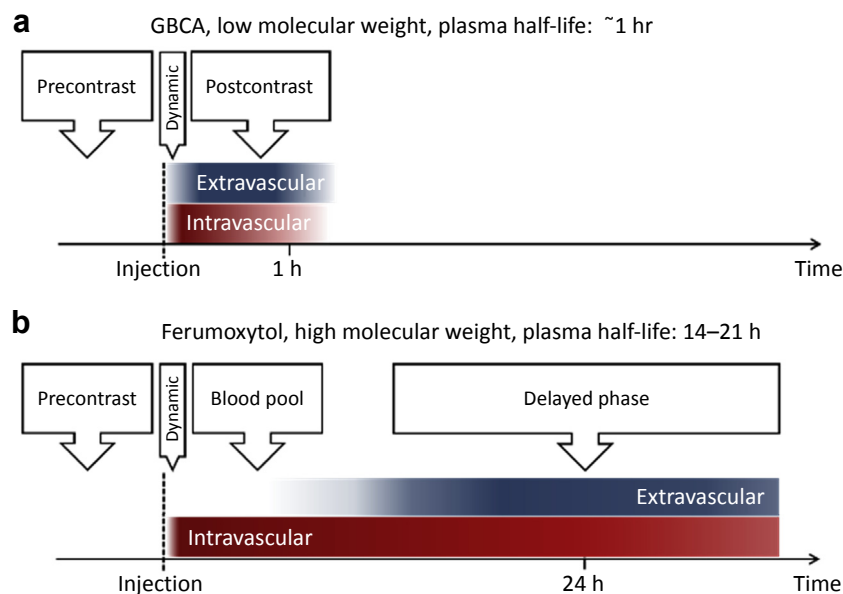


**Figure 1 | Phases of (a) gadolinium-based contrast agents (GBCAs) and (b) ferumoxytol enhancement.** Unlike GBCAs, ferumoxytol has a long intravascular half-life that results in a long blood pool phase prior to detectable contrast extravasation. Images provided courtesy of Edward A. Neuwelt.

print & web 4C/FPO

warning, which highlighted potential fatal and serious hypersensitivity reactions, including anaphylaxis. The warning emphasized the importance of trained personnel, appropriate medications being readily available, and monitoring patients for at least 30 minutes following administration to properly screen for hypersensitivity reactions. In the 3 premarketing clinical trials of Feraheme,<sup>21–23</sup> including 1164 patients, the aggregate rate of anaphylaxis was 0.2%.<sup>14</sup> The postmarketing trials had even better results; the largest trial with 8666 patients showed a serious adverse event rate of 0.2% and an anaphylaxis rate of 0.02%.<sup>24</sup> Recently, several studies described the diagnostic use of ferumoxytol in MRI, with no serious adverse events being reported.<sup>20,25–34</sup> The frequency of ferumoxytol-related adverse events (10%–14.6%) and serious adverse events (0%–1%) were comparable in all investigations, with rates similar to those seen with ionic iodinated contrast agents, and were 10 times higher than gadolinium-related events.<sup>35</sup> The initial administration rate of a 510 mg bolus over 17 seconds was lowered to a slow infusion of 510-mg-diluted ferumoxytol over 15 minutes, as suggested by the FDA recommendation. By reducing the rate of administration, the frequency of these events may also be reduced.

Ferumoxytol has also shown an excellent safety profile in pediatric patients.<sup>20</sup> Typical doses of 1 to 5 mg/kg for imaging purposes are much lower than the therapeutic dose and do not have a significant effect on hemoglobin values.<sup>20</sup>

#### CNS MRI WITH FERUMOXYTOL

Table 2 and Figure 3 indicate the most commonly used imaging sequences in the CNS.

#### Intracranial neoplasms

The use of ferumoxytol in MRI of primary brain tumors has been extensively studied. While lesion visualization with ferumoxytol is generally similar to that with GBCAs, differences in enhancement patterns may help in the differential diagnosis. Perfusion MRI and steady-state blood volume mapping may improve tumor grading by identifying the most malignant area for surgical targeting and therapy monitoring.

**Lesion visualization.** Contrast-enhanced MRI is routinely performed for the diagnosis of brain tumors, where the enhancement is the marker of the blood-brain barrier breakdown. Because extravasation of large molecules is slow, parenchymal enhancement is best seen in the delayed phase, 24 hours following ferumoxytol injection.<sup>15</sup> Contrast enhancement found on various clinically used T1-weighted MRI sequences improves border delineation and enables assessment of lesion internal morphology (Figure 4).<sup>36,37</sup> In primary malignant brain tumors, contrast enhancement with ferumoxytol is comparable with GBCA enhancement. No significant differences were found in the number of enhancing masses when gadolinium MRI and ferumoxytol MRI were compared in various primary brain tumors and metastatic lesions.<sup>38</sup> Differences in GBCA and ferumoxytol enhancement size and intensity may be present,<sup>37</sup> and they may reflect the differences in pathology, contrast agent dose, or timing of imaging. No difference was found in the enhancement size with the 2 contrast agents in metastatic lesions<sup>38</sup> or untreated glioma patients.<sup>36</sup> Decreased signal on T2-weighted images in the delayed phase may indicate high local ferumoxytol concentration or retention in tumor-associated macrophages. Delayed T1 and T2 enhancement together may help differentiate extracellular iron (e.g., tumor



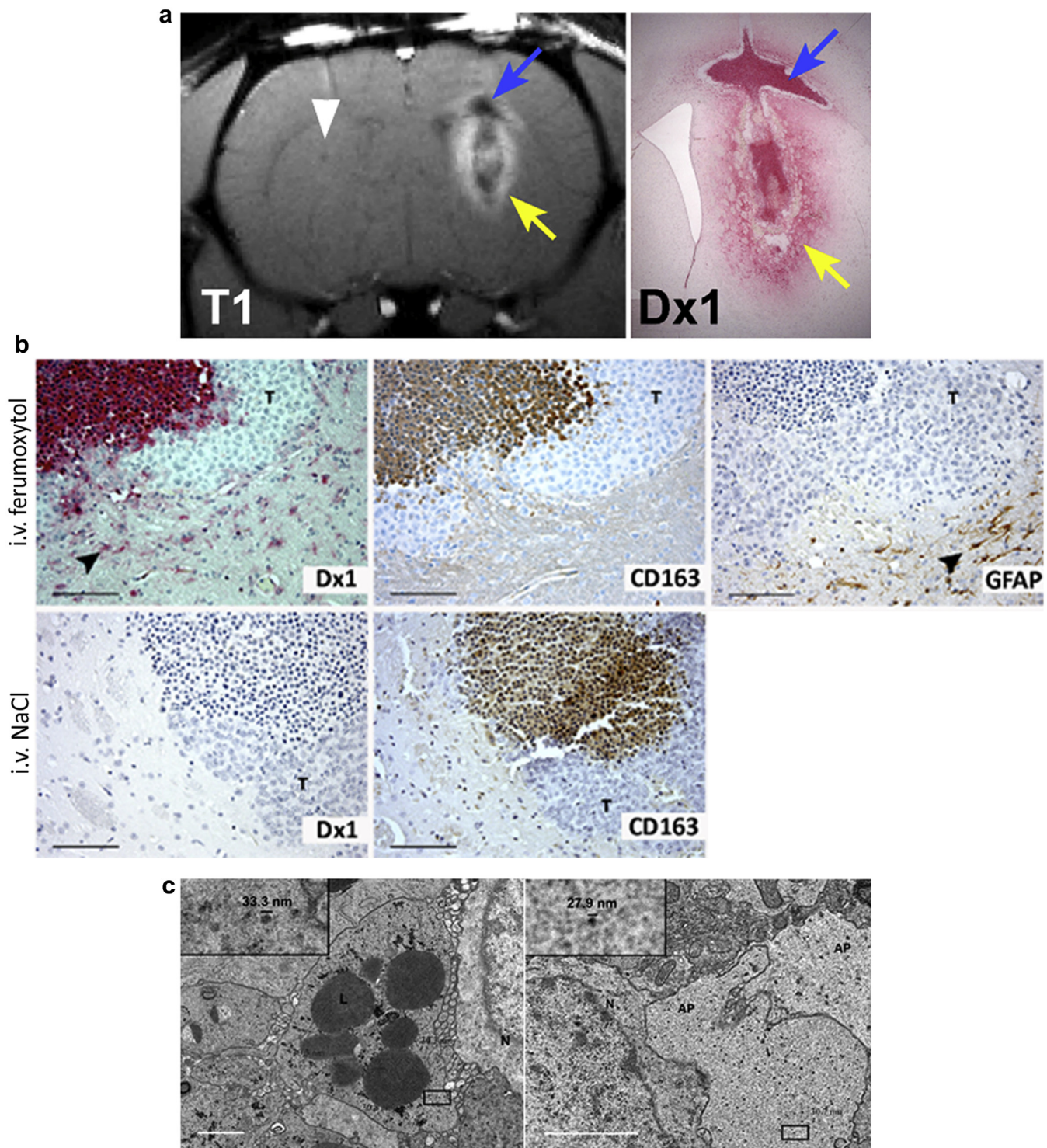


**Figure 2 | Ferumoxytol traffics from systemic circulation to reactive lesions: immunocompetent rat xenograft model demonstrating extravascular accumulation of ferumoxytol that correlates to the presence of activated macrophages.** (a) Enhancement of the magnetic resonance imaging (MRI) signal occurred in xenografted but not saline-injected hemispheres. Blue arrows indicate marked hypointense signal on T1 MRI that correlates with histologic findings of intense immunostaining of ferumoxytol in macrophages using dextran-1 (Dx1). Yellow arrows indicate typical hyperintense enhancement on T1 MRI that correlates with diffuse milder staining for ferumoxytol in the brain parenchyma and activated astrocytes using Dx1. White arrowhead indicates no signal change after saline injection in the contralateral control hemisphere. (b) Immunostaining demonstrates that ferumoxytol traffics from the systemic circulation to reactive central nervous system lesions. Immunostaining performed 48 hours after H460 non-small-cell lung carcinoma inoculation into caudate nucleus and 24 hours after i.v. ferumoxytol administration. A representative inflammatory lesion was immunostained with Dx1 to observe the ferumoxytol coating (red), cluster of differentiation (CD)163 for macrophages (brown), and glial fibrillary acidic protein (GFAP) for astrocytes (brown). All cell nuclei were counterstained with hematoxylin. T denotes live tumor cells. Arrowheads indicate reactive cells located outside of the main lesion. (Continued)

**Table 1 | Comparison between ferumoxytol and gadolinium**

Feature	Ferumoxytol	Gd-DTPA (Magnevist)
Basic element	Iron oxide	Gadolinium(III)
Molecular composition	Iron oxide coated with semisynthetic carbohydrate	Gadolinium chelated with diethylenetriamine penta-acetic acid
Relaxometric properties at 1.5 T/mM per s, 37°C in water	$r_1 = 15, r_2 = 89^{107}$	$r_1 = 3.3, r_2 = 3.9^{108}$
Elimination plasma half-life	14 h <sup>109</sup>	1.6 h
Relative size of the particle	Approximately 30 nm <sup>109</sup>	0.357 nm
Permeability to intact BBB	Minimal	Minimal
Typical times to peak enhancement (in brain lesions)	24 h <sup>110</sup>	3.5–25 min <sup>111</sup>
Signal change on T1-weighted sequence	Increased signal (signal decreased at very high concentrations)	Increased signal
Signal change on T2-weighted sequence	Decreased signal	Usually no change
Signal change on T2*-weighted sequence	Decreased signal	Decreased signal if given as a bolus
Distribution	Dynamic phase, blood pool phase, delayed phase (extra and intracellular)	Dynamic phase, extracellular phase
Imaging dose	1–7 mg/kg	0.1 mmol/kg
Excretion	Stored with the body's iron reserve and used in hemopoiesis coating with renal and fecal excretion	Renal
Boxed warning	Potential hypersensitivity	Potential NSF

BBB, blood-brain barrier; Gd-DTPA, gadolinium diethylenetriamine penta-acetic acid; NSF: nephrogenic systemic fibrosis.

necrosis) from intracellular iron (solid tumor).<sup>39</sup> T2\*-weighted scans in the blood pool phase have a potential added value to standard of care by improving the visualization of abnormal vasculature.<sup>40,41</sup>

**Differential diagnosis.** Dural-based–enhancing masses may represent benign or malignant diseases, and there is no method to effectively distinguish between these pathologies solely with GBCAs. Preliminary data suggest that delayed T1 enhancement with ferumoxytol may help distinguish between meningioma and dural metastases when used in addition to GBCA. While all dural metastases strongly enhanced with ferumoxytol and GBCAs, meningiomas showed poor to no enhancement with ferumoxytol (Figure 5).<sup>42</sup>

Tumefactive demyelinating lesions are large lesions usually accompanied by mass effect and abnormal enhancement, mimicking brain tumors, posing a particular diagnostic dilemma in patients with or without an established diagnosis of multiple sclerosis (MS).<sup>43</sup> Definitive diagnosis is given after surgery and histopathologic confirmation. A noninvasive marker is highly desirable to assess this diagnostic dilemma. Ferumoxytol uptake in inflammatory lesions appears on delayed T1- and T2-weighted images<sup>44</sup>; furthermore, perfusion MRI may help to differentiate tumors and demyelinating lesions, with relative cerebral blood volume (rCBV) being lower in tumefactive demyelinating lesions.

**Blood volume–based lesion assessment.** Measurement of the blood volume in tissues has important information

regarding the level of vascularization. Small molecular weight contrast agents can only estimate blood volume using a dynamic first-pass technique. An intravascular contrast agent enables the measurement of blood volume using a steady-state technique by calculating signal differences between pre- and postcontrast (intravascular) images. This has the benefit of high spatial resolution because rapid acquisition is not required.

Dynamic susceptibility contrast perfusion–derived or steady-state cerebral blood volume (CBV) maps reflect brain tumor malignancy by revealing hypervascular, highly perfused tumor regions. rCBV (relative to a normal reference region) has been shown to correlate with survival and facilitates preoperative diagnosis by differentiating low- and high-grade tumors.<sup>45</sup> Moreover, elevated rCBV values can predict the transformation of low-grade gliomas into high-grade tumors 12 months before T1 enhancement appears.<sup>46</sup> Although these studies were performed using GBCAs, ferumoxytol-derived rCBV values were in agreement with GBCA-derived values.<sup>10</sup>

High-grade gliomas, metastases, and to a lesser degree, primary CNS lymphomas exhibit high rCBV values with dynamic susceptibility contrast or steady-state imaging, which can help differentiate them from demyelination, abscesses, and toxoplasmosis.

**Intraoperative MRI and surgical targeting.** More aggressive, hypervascular tumor regions with high rCBV values are

**Figure 2 |** (Continued) Bar = 100  $\mu$ m. (c) Electron microscopy of a ferumoxytol-laden macrophage (left) and 2 astrocyte processes (right). Left image: iron oxide nanoparticles appear as electron-dense particles measuring approximately 30 nm in diameter located cytoplasmically and clustering around the lysosomes (L). Right image: 2 astrocyte processes (APs) showing dispersed, electron-dense ferumoxytol nanoparticles. N denotes neurons. Insets of both photos show a 27–33-nm diameter particle. Original magnification  $\times 6800$ ; bar = 1  $\mu$ m. Reprinted from *Nanomedicine: Nanotechnology, Biology, and Medicine*, volume 12, McConnell HL, Schwartz DL, Richardson BE, Woltjer RL, Muldoon LL, Neuwelt EA. Ferumoxytol nanoparticle uptake in brain during acute neuroinflammation is cell-specific, 1535–1542, 2016 with permission from Elsevier.

**Table 2 | Applications of ferumoxytol in central nervous system imaging**

MRI sequences		Use	Advantages	Disadvantages
Dynamic phase	DSC perfusion	DDx based on lesion vascularity Preoperative grading Prognosis assessment Biopsy guidance Therapy monitoring Progression versus pseudoprogression Detection of recurrence-malignant transformation Stroke or hemodynamic assessment	Low dose (1 mg/kg) needed No early contrast extravasation CBV, CBF, TTP, MTT, similar to CT-MRI (gadolinium) perfusion	Low spatial resolution Susceptibility artifacts, distortions Overestimation of large vessels (blooming) Bolus administration needed
Blood pool phase	T2*-weighted (GRE)	Improved visualization of abnormal vessels	Improved visualization of small abnormal vessels No bolus injection needed No post processing needed Part of most routine CNS protocols	Susceptibility artifact Motion sensitivity
	SS-CBV mapping (using pre- and post-Fe T2*w GRE scans)	DDx: ↑rCBV: HGG, PCNSL, metastasis ↓rCBV: LGG, demyelination, toxoplasmosis, abscess Preoperative grading Prognosis assessment Biopsy guidance Therapy monitoring Detection of recurrence-malignant transformation Progression versus pseudoprogression	High spatial resolution Thin slices, good 3D reformat for neuronavigation No distortions Full-brain coverage possible No bolus injection needed Not influenced by circulation parameters Repeatable Potentially quantitative	Susceptibility artifact Motion sensitivity Coregistration of the pre- and post-contrast images needed Time consuming based on coverage (5–10 min)
Delayed phase	T1 enhancement (SE or MPRAGE) High SI	Lesion visualization Assessment of BBB damage DDx: meningioma versus metastasis Intraoperative lesion assessment Post-Sx residual tissue assessment without additional CA injection Differentiating intra- and extracellular iron <sup>39</sup>	Potential alternative to GBCAs Similar enhancement patterns as gadolinium in most pathologies Prolonged enhancement (intra- and postoperative imaging without additional contrast agent administration) Prolonged enhancement May indicate intracellular uptake of ferumoxytol	Additional scanning needed 24 h following ferumoxytol administration High concentration of ferumoxytol may result in T1 signal drop If enhancement persists it may mimic intracerebral blood
	T2 enhancement (T2w TSE) Low SI	Assessment of BBB damage dg: meningioma versus metastasis Intraoperative lesion assessment Improved biopsy targeting Differentiating intra- and extracellular iron		Additional scanning needed 24 h following ferumoxytol administration If enhancement persists it may mimic intracerebral blood May be difficult to differentiate between intracellular iron and high concentration interstitial iron

BBB, blood-brain barrier; CA, contrast agent; CBF, cerebral blood flow; CBV, cerebral blood volume; CNS, central nervous system; CT, computed tomography; DDx, differential diagnosis; dg, diagnosis; DSC, dynamic susceptibility contrast; Fe, ferumoxytol; GBCA, gadolinium-based contrast agent; GRE, gradient echo; HGG, high-grade glioma; LGG, low-grade glioma; MPRAGE, magnetization-prepared rapid gradient-echo; MRI, magnetic resonance imaging; MTT, mean transit time; PCNSL, primary central nervous system lymphoma; rCBV, relative cerebral blood volume; SE, spin echo; SI, signal intensity; SS-CBV, steady-state cerebral blood volume; Sx, surgery; T2 TSE, T2-weighted turbo spin echo; T2\*w, T2\*-weighted; TTP, time to peak; 3D, 3-dimensional.

the optimal sites for biopsy and can be identified using dynamic or steady-state perfusion imaging with ferumoxytol. However, dynamic perfusion methods have limited ability to differentiate between vessels and high tissue CBV, which compromises the assessment of small active tumor hotspots that could be the source of subsequent tumor progression and short survival. Because of its near distortion-free high-resolution images, steady-state CBV mapping can overcome this limitation and may enable more precise targeting (Figure 6). Late T2 enhancement with ferumoxytol has also been described to mark specific tumor areas and may again be useful for accurate biopsy targeting.<sup>44</sup> Finally, delayed enhancement with ferumoxytol enables intra- and post-operative assessment of a residual tumor without injecting additional contrast agent.

**Treatment monitoring.** After brain tumor therapy with radiation or chemoradiotherapy, an increased edema and

contrast enhancement on MRI may either represent tumor progression (growing tumor mass, indicating failure of ongoing therapy) or pseudoprogression, which is defined as a treatment-induced subacute inflammatory reaction without underlying tumor growth.<sup>47</sup> Differentiating pseudoprogression from true tumor progression is a significant clinical problem. Response assessment according to the currently standard Response Assessment in Neuro-Oncology criteria is based on morphology and contrast enhancement and may delay or prevent proper therapy.<sup>48</sup> Similarly, antiangiogenic drugs affect the blood-brain barrier permeability without decreasing the tumor mass itself, which can lead to a pseudoresponse<sup>49</sup> that cannot be differentiated from a true response with the Response Assessment in Neuro-Oncology criteria. It is becoming apparent that a phenomenon similar to pseudoprogression occurs after an immune checkpoint blockade for cancer therapies.<sup>50</sup> This has led to the



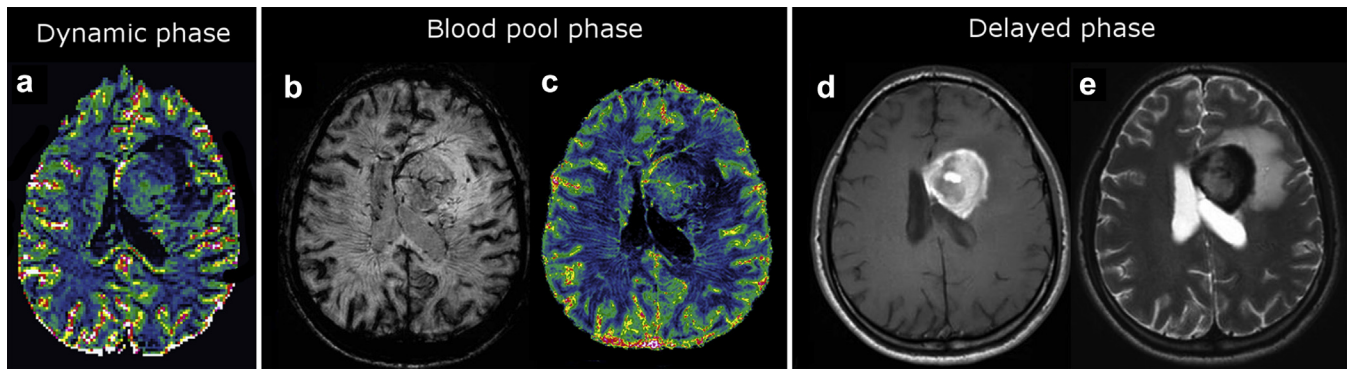


**Figure 3 | Possible sequences of ferumoxytol in the central nervous system during the (a) dynamic, (b,c) blood pool, and (d,e) delayed phases after administration in a patient with newly diagnosed primary central nervous system lymphoma. (a)** Cerebral blood volume (CBV) map calculated from dynamic susceptibility contrast perfusion with ferumoxytol shows mildly elevated relative CBV in the neoplasm. **(b)** Susceptibility-weighted image shows curvilinear branching hypointensities compatible with abnormal tumor vasculature. **(c)** Steady-state CBV map with a high resolution shows increased blood volume. **(d)** Axial T1 magnetic resonance imaging (MRI) demonstrates a typical enhancement 24 hours after ferumoxytol administration. **(e)** Axial T2 MRI shows marked hypointensity in the tumor 24 hours after ferumoxytol administration. Reprinted with permission from Neuwelt EA, Várallyay CG, Manninger S, et al. The potential of ferumoxytol nanoparticle magnetic resonance imaging, perfusion, and angiography in central nervous system malignancy: a pilot study. *Neurosurgery*. 2007;60:601–611; discussion 11–12.<sup>15</sup> Copyright © Oxford University Press.

development of immune-related response criteria to better identify cases of pseudoprogression,<sup>51</sup> although these criteria are not specific to the CNS. According to the immune-related Response Assessment in Neuro-Oncology criteria published in 2015, patients who have imaging findings that meet the Response Assessment in Neuro-Oncology criteria for progressive disease within 6 months of starting immunotherapy should undergo a confirmation of follow-up imaging (in 3 months) before defining the patients as nonresponsive to treatment.<sup>52</sup> The use of CBV mapping with ferumoxytol may help determine therapeutic efficacy in a variety of CNS tumors by differentiating highly vascular malignant tumor tissue from treatment-related neuroinflammation, which correlates with survival (Figures 7 and 8).<sup>10,53</sup>

We can now obtain high-resolution steady-state CBV images that differentiate regions of high vascularity and active tumor growth.<sup>10,13</sup> Steady-state blood volume mapping with ferumoxytol is particularly helpful for imaging cortical lesions with an improved spatial resolution.

#### Neuroinflammation and demyelination

Delayed imaging with ferumoxytol allows the assessment of inflammation as an imaging biomarker. Few human MS investigations have been performed using ferumoxytol, but studies using other USPIOs such as ferumoxtran-10 have identified MS lesion phenotypes with the following enhancement patterns: (i) GBCA+/delayed USPIO enhancement (USPIO+), (ii) GBCA+/USPIO-, and (iii)

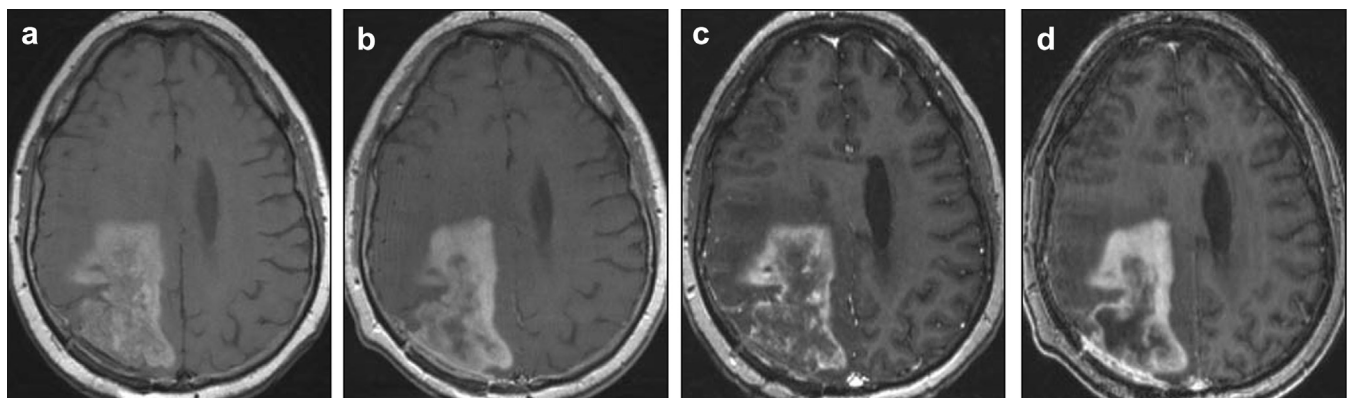
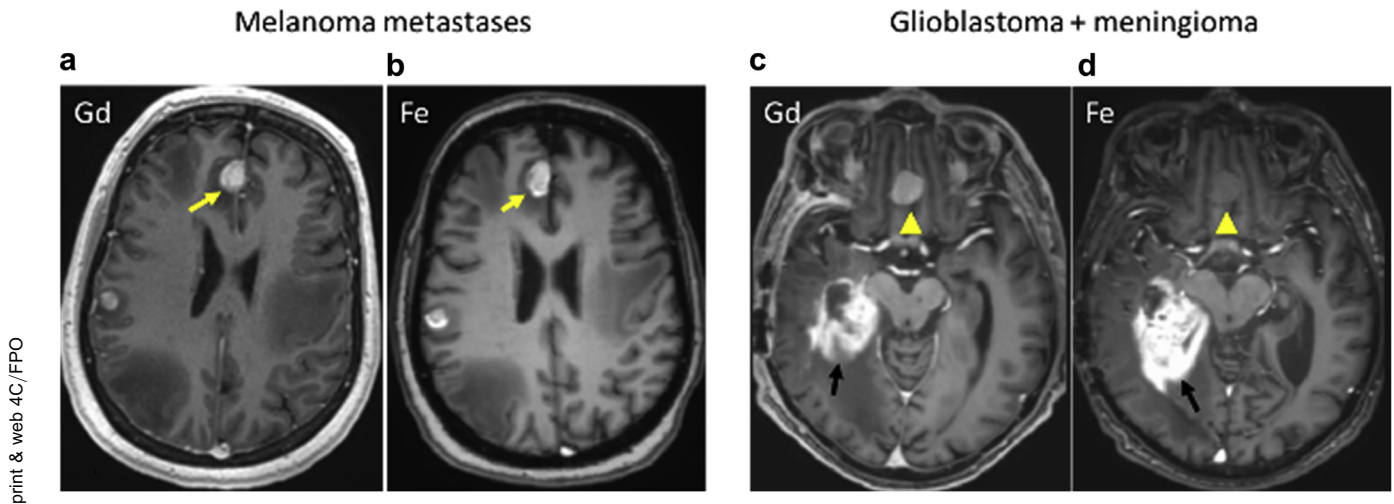


**Figure 4 | Axial brain magnetic resonance image (MRI) of a 19-year-old man who underwent previous radiation and chemotherapy for glioblastoma multiforme, with a clinical suspicion for pseudoprogression. (a)** Spin-echo (SE) T1 MRI obtained 24 hours after ferumoxytol administration shows moderately intense enhancement. **(b)** SE T1 gadoteridol-enhanced MRI shows concordant enhancement size and intensity. **(c)** Magnetization-prepared rapid gradient-echo (MPRAGE) MRI performed 24 hours after ferumoxytol administration shows a moderate (although less homogeneous) enhancement intensity compared with the SE image. **(d)** Gadoteridol-enhanced MPRAGE scan shows a more homogeneous and greater enhancement intensity than the ferumoxytol-enhanced MPRAGE scan. The administered ferumoxytol dose was 510 mg. From Hamilton BE, Nesbit GM, Dosa E, et al. Comparative analysis of ferumoxytol and gadoteridol enhancement using T1- and T2-weighted MRI in neuroimaging. *AJR Am J Roentgenol*. 2011;197:981–988,<sup>36</sup> used with permission from *AJR Am J Roentgenol*.



print &amp; web 4C/FPO

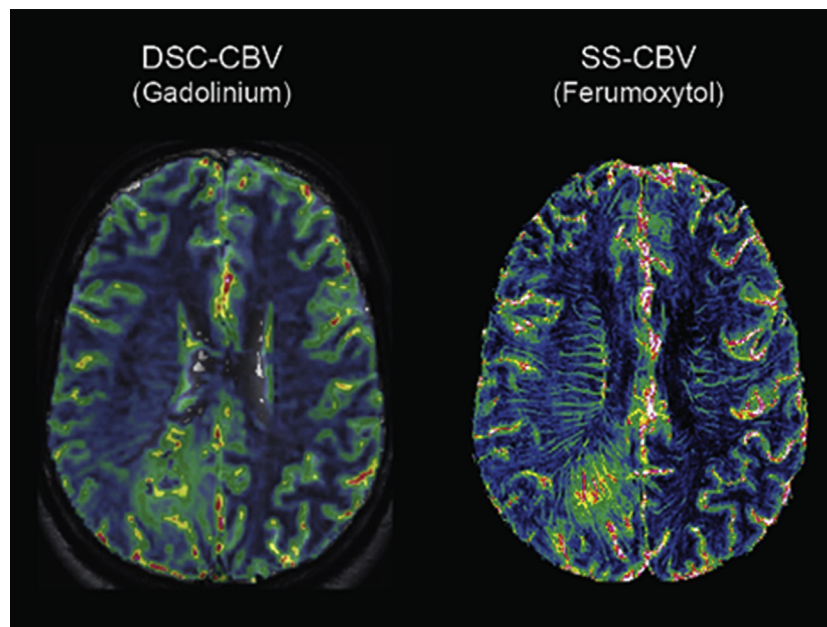
**Figure 5 | Axial T1-weighted postcontrast magnetic resonance images in 2 different patients with similar-appearing frontal midline lesions.** (a,b) The mass (yellow arrows) is similarly enhanced by both gadolinium (Gd) and ferumoxytol (Fe) in a patient with melanoma metastases. A meningioma (yellow arrowheads) only enhances with Gd (c) and not Fe (d). Of note, the glioblastoma in the same images (black arrows) enhances avidly with both agents. Images provided courtesy of Edward A. Neuwelt.

GBCA-/USPIO+. The USPIO-specific lesions are of particular interest because they represent endothelial activation and diapedesis without blood-brain barrier disruption. Longitudinal studies demonstrate that in a fraction of GBCA-/USPIO+ MS lesions, delayed USPIO preceded GBCA enhancement by 1 month, suggesting extensive monocyte-macrophage extravasation in MS.<sup>54</sup>

Ferumoxytol has been used to study neuroinflammatory processes associated with Japanese macaque encephalomyelitis,<sup>55</sup>

a demyelinating disease of the nonhuman primate with strong similarities to MS.<sup>56</sup> A study by Tagge *et al.*<sup>55</sup> demonstrated substantially greater USPIO+ lesion volume than GBCA+ lesion volume during the acute Japanese macaque encephalomyelitis disease phase, indicating spatially and temporally extensive monocyte-macrophage migration into the CNS.

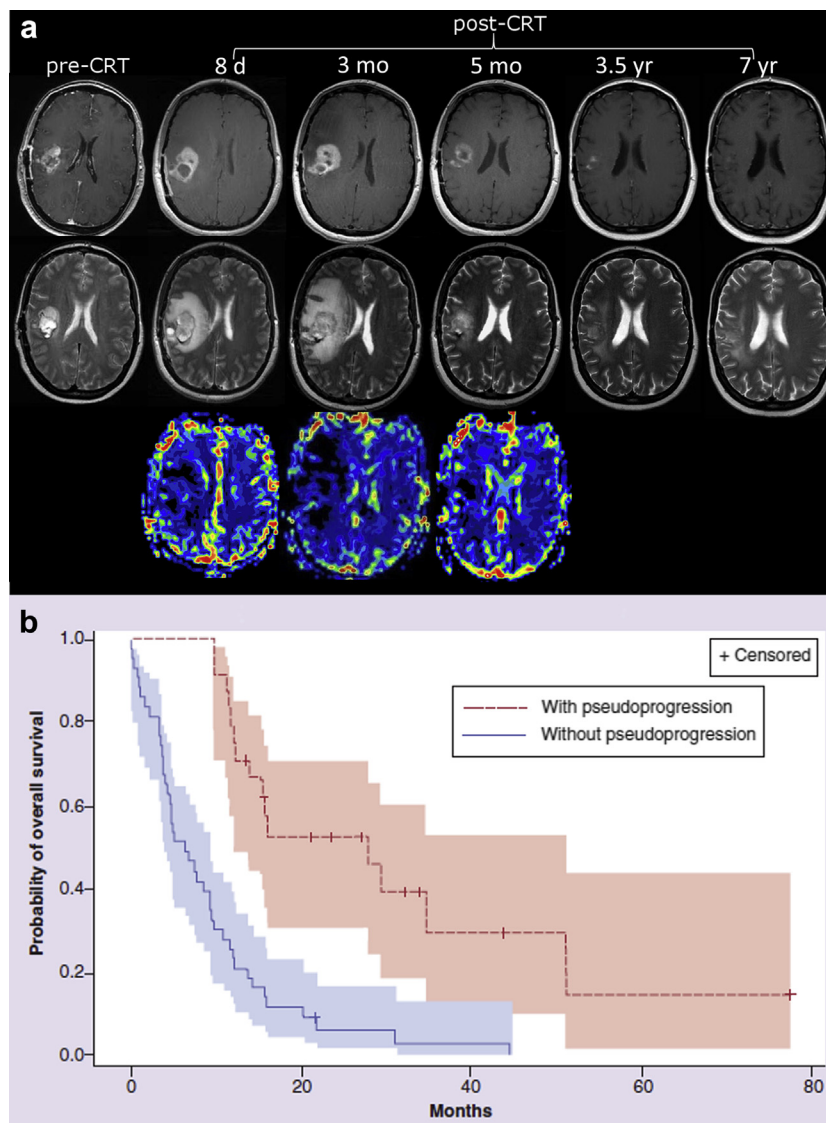
Farrell *et al.*<sup>44</sup> demonstrated delayed enhancement with ferumoxytol in patients with MS, primary CNS lymphoma, posttransplant lymphoproliferative disorder, acute



print &amp; web 4C/FPO

**Figure 6 | Steady-state cerebral blood volume (SS-CBV) maps using ferumoxytol offer higher spatial resolution and allow better identification of hypervascular areas for surgical targeting in glioblastoma patients.** Compare the spatial resolution of CBV map using dynamic susceptibility contrast (DSC) perfusion-weighted imaging with a standard dose of gadolinium (DSC-CBV) (left) and the SS ferumoxytol CBV map (right) using ferumoxytol (3 mg/kg). The scan on the right more clearly demonstrates a central hypervascular area in the right occipital hemisphere with the greatest vascularity, which is likely the most malignant portion of the tumor. Images provided courtesy of Edward A. Neuwelt.





print &amp; web 4C/FPO

**Figure 7 | Pseudoprogession can be diagnosed using perfusion magnetic resonance imaging (MRI) with ferumoxytol and correlates with overall survival.** (a) Axial MRIs of a 47-year-old woman with glioblastoma. The patient underwent T1-weighted sequences after gadolinium administration, and T2-weighted postoperative images prior to chemoradiotherapy (CRT) are shown. Eight days after CRT completion, the patient's scans showed radiographic worsening, followed by further deterioration on follow-up MRI while the patient continued to receive adjuvant temozolomide chemotherapy. Although the updated Response Assessment in Neuro-Oncology criteria would indicate a true tumor progression, the blood volume of the lesion was low on ferumoxytol dynamic susceptibility contrast cerebral blood volume maps, which instead indicates pseudoprogession. The patient received only 3 courses of bevacizumab and continued adjuvant temozolomide. Substantial improvement is seen on the 5-month follow-up MRI after the completion of bevacizumab therapy. Seven years after the completion of CRT, the image indicates that the patient is stable without evidence of recurrence-progression (the patient is still on adjuvant temozolomide chemotherapy). (b) Kaplan-Meier estimates of overall survival with respect to the presence or absence of pseudoprogession. From Gahramanov S, Varallyay C, Tyson RM, et al. Diagnosis of pseudoprogession using MRI perfusion in patients with glioblastoma multiforme may predict improved survival. *CNS Oncol.* 2014;3:389–400.<sup>53</sup> Reproduced with permission of Future Medicine in the format Journal/magazine via Copyright Clearance Center.

disseminated encephalomyelitis (Figure 9), and chronic encephalitis; a higher number of lesions are visible with ferumoxytol than with GBCAs.

Future applications (ultrahigh field MRI [Figure 10 shows an example how ferumoxytol improves the visualization of cerebral microvasculature at 7 T field strength], seizure imaging, functional MRI, and vascular imaging in the CNS) can be found in Supplementary Material 1.

## BODY IMAGING WITH FERUMOXYTOL

### Liver and spleen

Metastases are the most common solid liver lesions (although benign hepatic hemangiomas are also frequent), and MRI is considered to be the definitive tool for differentiating these entities in an oncological setting. However, this task can be difficult when lesions are small or when hemangiomas are atypical or of the sclerosing subtype. In many cases,

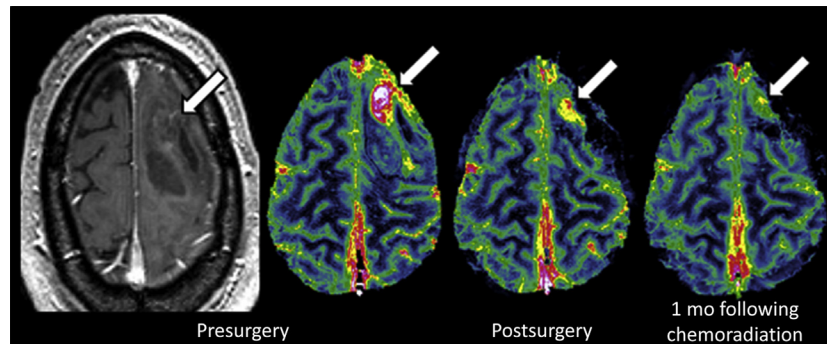


**Figure 8 | A 42-year-old male patient with glioblastoma.** The T1-weighted postgadoteridol administration scan shows no-to-minimal enhancement. In contrast, a highly vascular area (arrows) is seen on high-resolution steady-state cerebral blood volume (CBV) maps obtained with ferumoxytol. Residual tumor with high CBV shows reduction following chemoradiotherapy (postsurgery scan), with a continued decrease 1 month following chemoradiotherapy, indicating a treatment response. Images provided courtesy of Edward A. Neuwelt.

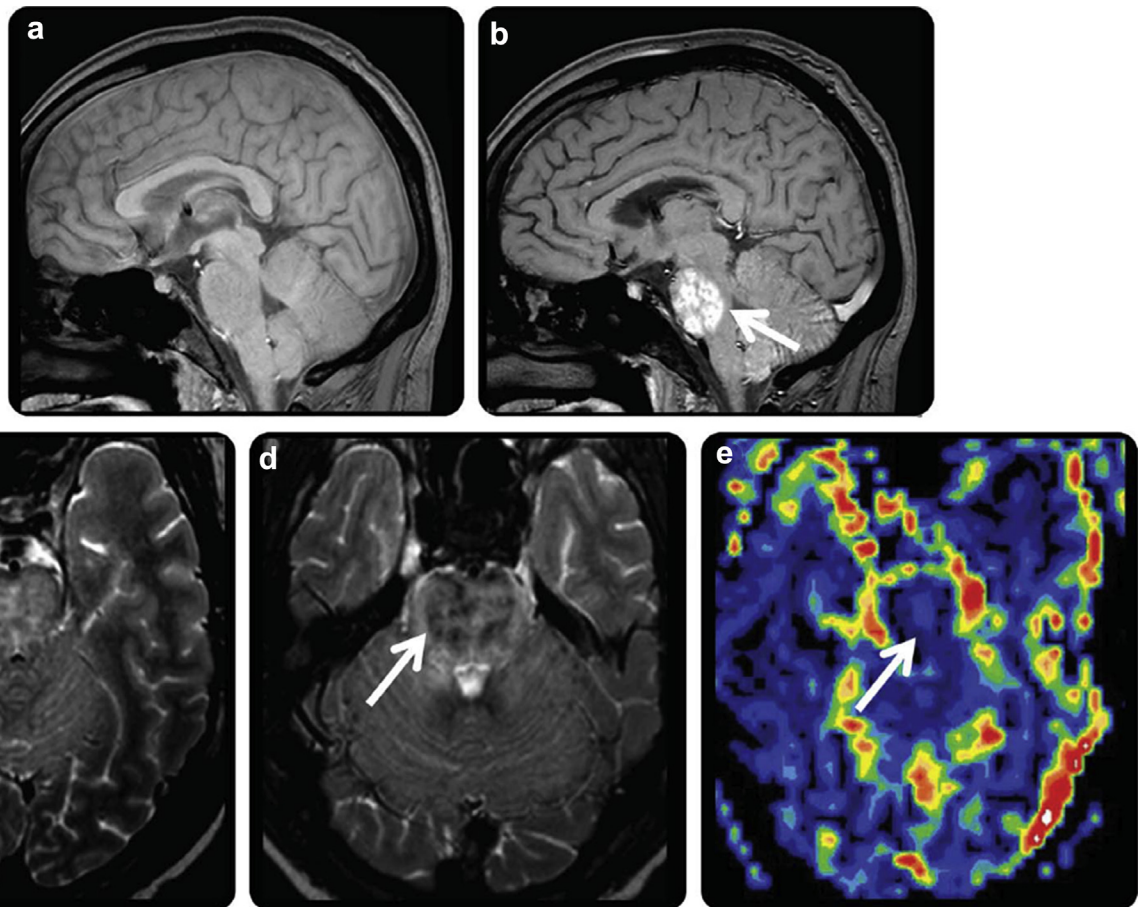


**Figure 9 | A patient with suspected pontine glioma was diagnosed with pontine demyelination using ferumoxytol.** (a) The pre-contrast T1-weighted imaging shows little abnormality. (b) A T1-weighted sagittal magnetic resonance image (MRI) 24 hours following ultrasmall superparamagnetic iron oxide administration shows diffuse intense enhancement because of ferumoxytol uptake in the pons (arrow). (c) An axial noncontrast T2-weighted MRI shows a patchy nonspecific increased T2 signal within the pons (arrow). (d) An axial T2-weighted MRI obtained 24 hours following ferumoxytol administration shows patchy hypointensities in the pons (arrow) correlating with ferumoxytol uptake. (e) A ferumoxytol-based dynamic susceptibility contrast perfusion image shows low relative cerebral blood volume centrally within the pons (arrow) corresponding to the area of enhancing abnormality that is similar to normal-appearing white matter, a finding supportive of demyelination rather than high-grade primary central nervous system neoplasm. From Farrell BT, Hamilton BE, Dosa E, et al. Using iron oxide nanoparticles to diagnose CNS inflammatory diseases and PCNSL. *Neurology*. 2013;81:256–263,<sup>44</sup> used with permission from *Neurology*.

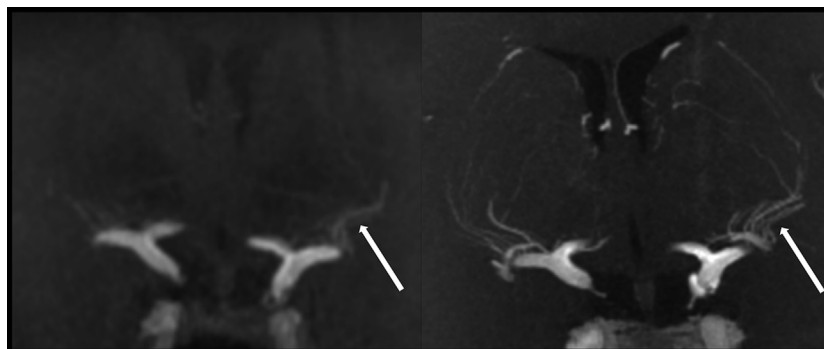


**Figure 10 | Ferumoxytol magnetic resonance angiography (MRA) improves visualization of cerebral microvasculature when compared with gadolinium MRA at 7T field strength.** Gadolinium-enhanced 3-dimensional T1-weighted gradient-echo volumetric interpolated brain examination MRA of the supraclinoid internal carotid arteries (left) shows faint visualization of lenticulostriate vessels (white arrows). Ferumoxytol-enhanced MRA (right) demonstrates markedly improved visualization of the lenticulostriate microvasculature (white arrows). Images provided courtesy of Ramon Barajas.

small hemangiomas can be differentiated from other lesions based on the retention of intravascular contrast agents such as gadofosveset trisodium or ferumoxytol on delayed scans.<sup>57,58</sup>

Significant negative (hypointense) T2 enhancement of normal liver parenchyma is seen within 10 minutes of i.v. ferumoxytol administration. Because ferumoxytol is taken up by the MPS, it has the potential to serve as a tool for measuring MPS dysfunction. Quantitative measures of MPS function, as estimated using dynamic imaging of ferumoxytol uptake in the liver, may prove to be useful predictors of graft dysfunction and rejection, although validations in humans are still pending.<sup>59</sup>

### Pancreas

Computed tomography (CT) is the imaging method of choice for pancreatic diseases, including pancreatic adenocarcinoma, pancreatitis, and neuroendocrine tumors of the pancreas. MRI of the pancreas holds significant promise secondary to the many inherent contrast mechanisms, particularly those with novel contrast agents.

Blood vessel density is known to be markedly lower in pancreatic ductal adenocarcinoma compared with that in other malignancies,<sup>60</sup> which may explain its poor response to antiangiogenic therapies, thus making pancreatic ductal adenocarcinoma a poor choice for interrogation with dynamic techniques. Because of the long intravascular blood pool residence time, iron oxide nanoparticles offer a steady-state solution for the precise measurements of microvascular parameters, as demonstrated in preclinical studies,<sup>61–64</sup> and are better imaging agents for pancreatic ductal adenocarcinoma. In subcutaneous xenograft models, MRI of magnetic nanoparticles provides a noninvasive, accurate assessment of fractional blood volume and vessel size index.<sup>62–72</sup>

The delayed uptake of magnetic nanoparticles by macrophages<sup>73</sup> has also been a focus of MRI for multiple applications in the pancreas, including improved delineation of pancreatic adenocarcinoma,<sup>17</sup> and for quantifying inflammation in patients with early onset type 1 diabetes (Figure 11).<sup>74,75</sup>

### Staging of malignant tumors

The current anatomic imaging techniques for nodal staging (e.g., CT and MRI) rely on morphologic lymph node characteristics such as size, shape, and morphology, but sensitivity for differentiating malignant lymph nodes from benign ones remains low.<sup>76</sup> Sensitivity could be improved using USPIOs; however, most of the available data have been obtained with USPIOs other than ferumoxytol.<sup>77,78</sup> Iron oxide particles are taken up by and retained in normal lymph nodes, resulting in signal loss on T2- and T2\*-weighted images (Figure 12).<sup>79</sup> When nodes are infiltrated with malignant cells, the nodal USPIO nanoparticle uptake capacity reduces and malignant nodes retain high signal intensity on T2\*-weighted images. Optimal node T2\*-weighted imaging contrast with ferumoxytol can be achieved 24 to 48 hours following injection (Figures 12 and 13).<sup>16,79</sup>

### Prostate

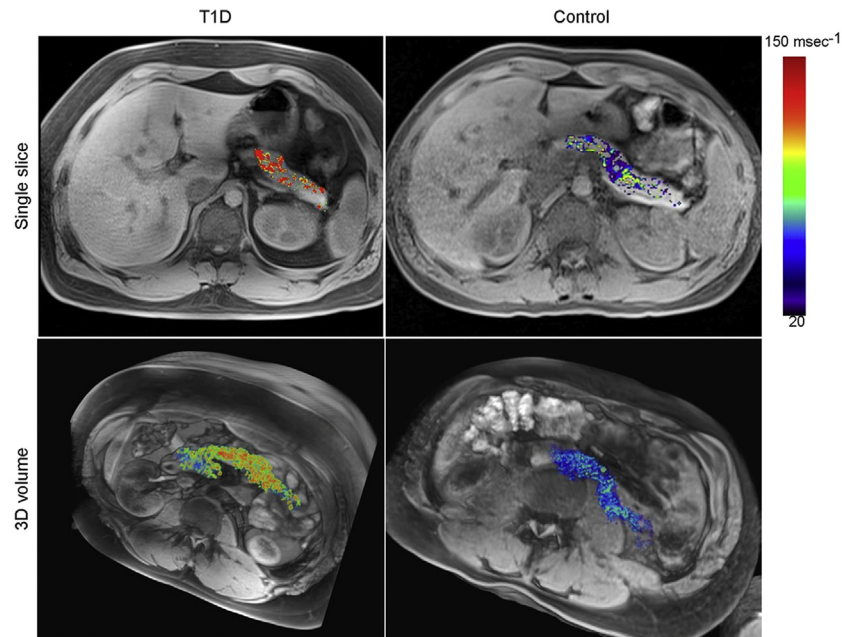
Nodal involvement is noted in 5% to 10% of patients with prostate carcinoma, but the detection sensitivity of CT and MRI remains lower than 30%.<sup>80</sup>

Clinical experience with ferumoxytol-enhanced MRI for mapping metastatic lymph nodes in patients with prostate cancer is limited. Harisinghani *et al.*<sup>16</sup> reported a significant decrease in the signal-to-noise ratio in benign nodes on T2\*-weighted images but little change in the signal-to-noise ratio in malignant nodes using ferumoxytol at a dose of 4 mg/kg. MRI was performed before and 5, 18, and 24 hours after ferumoxytol injection. The most appropriate dose of ferumoxytol is uncertain because lymph nodes in the pelvis are heterogeneous. Turkbey *et al.*<sup>81</sup> found that a higher dose of i.v. ferumoxytol (up to 7.5 mg/kg) was needed to completely darken the normal pelvic nodes compared with ferumoxtran-10.

Direct injection of ferumoxytol into the prostate (lymphography) has shown promise in mapping sentinel lymph nodes, as demonstrated in nonhuman primates.<sup>82</sup>

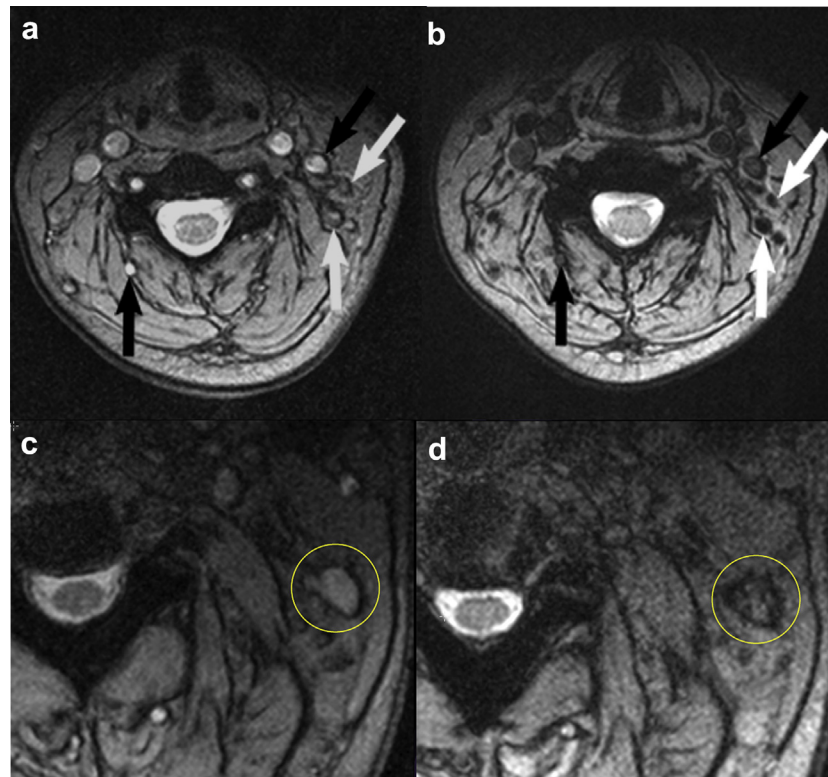
Other potential applications in body imaging (breast and sentinel lymph node, colorectal, and adrenal gland MRI and












print &amp; web 4C/FPO

**Figure 11 | Increased pancreatic nanoparticle accumulation in patients with type 1 diabetes (T1D).** Single-slice (upper row) and 3-dimensional (3D) volume sets (lower row) of a representative patient with recently diagnosed T1D (left) and a normal control subject (right). From Gaglia J, Harisinghani M, Aganj I, et al. Noninvasive mapping of pancreatic inflammation in recent-onset type-1 diabetes patients. *Proc Natl Acad Sci U S A.* 2015;112:2139–2144,<sup>75</sup> used with permission of *Proc Natl Acad Sci U S A.*



print &amp; web 4C/FPO

**Figure 12 | Benign (a,b) and malignant (c,d) nodal patterns.** Axial T2\*-weighted gradient-echo (GRE) pre-ferumoxytol scan (a) shows intranodal high signal (white arrows) compared with hypointensity at 24 hours post ferumoxytol scan (b), indicative of normal lymph nodes. The white arrows in (a) indicate cervical lymph nodes. Axial T2\*-weighted GRE scan shows a normal, high pre-contrast intranodal signal (circle, c) compared with internal intranodal speckling (circle, d) suggesting a pathologic lymph node (black arrows indicate vascular structures). Images provided courtesy of Bronwyn E. Hamilton.

No.	Postdose	Description	Diagnosis
#1		No blackening of node or node is hyperintense to surrounding tissue; heterogeneous or homogenous architecture	Metastatic
#2		Node has central high signal with darkening along the peripheral rim; heterogeneous architecture	Metastatic
#3		Partial darkening whereby more than 50% of the node has an area of high signal intensity; heterogeneous architecture	Metastatic
#4		Less than 50% of node has high signal intensity; heterogeneous architecture	Possibly metastatic
#5		Node having an overall dark signal other than a central or hilar area of fat seen on T1 sequence; heterogeneous architecture	Nonmetastatic
#6		Node having an overall dark signal with speckles of subtle granularities; homogenous architecture	Nonmetastatic
#7		Node having an overall dark signal intensity; homogenous architecture	Nonmetastatic

**Figure 13 | Lymph nodes with an area of high signal intensity, which encompasses the entire node or a large portion of it, are considered metastatic.** A node with fatty hilum, complete signal void, and speckles of granularity without a definite focus of high signal intensity is considered nonmetastatic. From Anzai Y, Piccoli CW, Outwater EK, et al. Evaluation of neck and body metastases to nodes with ferumoxtran 10-enhanced MR imaging: phase III safety and efficacy study. *Radiology*. 2003;228:777–788,<sup>79</sup> used with permission from *Radiology*.

stem cell labeling) can be found in the [Supplementary Material 1](#).

### Inflammation

Focal inflammation can mimic neoplasia. By labeling macrophages with ferumoxytol *in vivo*, macrophage trafficking can be detected and inflammatory lesions can be localized.<sup>83,84</sup>

Ferumoxytol-enhanced MRI is promising for assessing rheumatologic diseases and differentiating acute from chronic inflammatory kidney disease.<sup>85–88</sup> Ferumoxytol-enhanced MRI has also been used for diagnosing osteomyelitis in the feet of patients with diabetes (Figure 14)<sup>89</sup> and for assessing the activity of Crohn's disease.<sup>90</sup>

### Pediatric MRI with ferumoxytol

Using ferumoxytol as an MRI agent in the pediatric population has similar potential benefits as those observed in adults. Specific advantages include separation of i.v. cannula placement/ferumoxytol administration from the MRI scanning itself (which may improve the cooperation of the child if MRI is performed without anesthesia).<sup>32</sup> For pediatric brain tumor patients undergoing MRI with anesthesia, gadolinium and ferumoxytol in a single imaging session was well tolerated.<sup>33</sup> Three-dimensional contrast-enhanced MR angiography (MRA) applications in pediatric CKD patients have been reported to evaluate i.v. access placement, vascular thrombosis, cardiac and renal transplantation anastomosis, re-transplantation, and biliary/liver dysfunction, thereby eliminating concerns about nephrogenic systemic fibrosis.<sup>30,91</sup> Finally,

ferumoxytol may provide a higher level of confidence for the delineation of small vessels prior to surgery in body MRA.<sup>32</sup>

Many types of lymphomas, soft tissue sarcomas, and bone sarcomas are staged with 18F-fluorodeoxyglucose positron emission tomography (18F-FDG-PET)/CT.<sup>92</sup> To provide a radiation-free alternative, whole-body diffusion-weighted MRI has been developed without the use of contrast agents. However, the use of ferumoxytol with this technique may be advantageous (Figure 15).<sup>28</sup>

### VASCULAR MRI WITH FERUMOXYTOL

Traditional contrast-enhanced MRA employs timed, first-pass imaging of a gadolinium bolus, focused on the arterial or venous territory of interest. For the majority of GBCAs, the volume of distribution is the extracellular fluid space, which is quickly accessed after the arterial first pass. Therefore, the time window for a pure or predominantly vascular phase is very short, and the acquisition can be technically challenging. Gadofosveset is a GBCA with an extended blood residence time because of reversible binding to serum albumin. However, compared with ferumoxytol, gadofosveset has a much shorter intravascular half-life (30 minutes vs. 14–21 hours), and at any given time, approximately 20% of gadofosveset is distributed in the extracellular fluid space. Moreover, gadofosveset is being withdrawn from production such that by the end of 2016, ferumoxytol will be the only intravascular MRI contrast agent available for human use in the US.

Imaging in patients with a vascular disease is challenging; many (20%–30%) patients are diabetic with associated

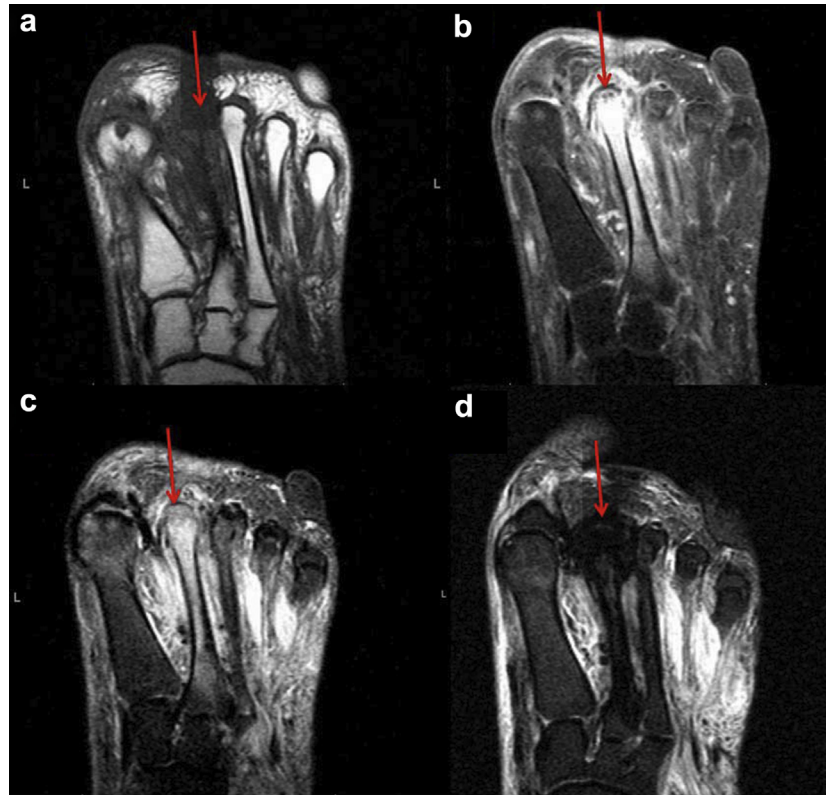


**Figure 14 | Second metatarsal osteomyelitis (arrows) in a 25-year-old patient with a history of a shotgun injury on the foot.** T1-weighted noncontrast magnetic resonance imaging (MRI) (a) shows a hypointense signal involving the second metatarsal (red arrow) and marked enhancement on gadolinium-enhanced T1-fat suppressed MRI. (b) Noncontrast T2-weighted MRI shows edema in the second metatarsal (red arrow) and surrounding soft tissues. (c) T2-weighted MRI obtained 14 hours following ferumoxytol administration. (d) Marked hypointensity compatible with ferumoxytol uptake and consistent with the diagnosis of osteomyelitis. From Neuwelt A, Langsjoen J, Byrd T, et al. Ferumoxytol negatively enhances T2-weighted MRI of pedal osteomyelitis in vivo [e-pub ahead of print]. *J Magn Reson Imaging*. 2017;4:1241-1245.<sup>88</sup> used with permission from *J Magn Reson Imaging*.

print & web 4C/FPO

difficult vein access<sup>93</sup> and many (20%–40%) have CKD, which can prohibit the use of iodine- and gadolinium-based contrast agents.<sup>34,94</sup> Ferumoxytol is a very attractive option in these patients and can be used without the need for bolus timing or complex image acquisition schemes. Ferumoxytol's excellent safety profile has already been established in patients with chronic renal insufficiency, although it must always be used with close physiological monitoring.

In recent years, there have been several reports regarding the successful use of ferumoxytol in vascular imaging in adults and children with renal failure.<sup>30,32,34,57,91,95,96</sup> The studies suggest that ferumoxytol provides similar or improved quality images compared with GBCAs, without the concerns of long-term gadolinium accumulation.<sup>1–4</sup> Some of the potential applications of ferumoxytol in vascular imaging are summarized in Table 3.

### Cardiac imaging

To date, there have been very few reports regarding the use of ferumoxytol in patients with ischemic heart disease. In patients with acute myocardial infarction, Alam *et al.*<sup>97</sup> and Yilmaz *et al.*<sup>98</sup> showed macrophage activation in injured

myocardium. These authors exploited the effects of ferumoxytol in causing signal loss owing to its effect on T2 values and did not address vascular enhancement because of the shortening of T1 values.

In congenital heart disease, accurate anatomic assessment is important for surgical or interventional planning. Conventional first-pass MRA and 2-dimensional cardiac cine methods provide limited definition of intracardiac structures. In contrast, ferumoxytol supports the acquisition of 4-dimensional images of the beating heart with 4-dimensional, multiphase, steady-state imaging with contrast enhancement (Figure 16).<sup>99</sup> Similarly, comprehensive motion-compensated highly accelerated 4-dimensional flow MRI with ferumoxytol enhances the quality of 4-dimensional flow information with reduced respiratory motion artifacts in children with congenital heart disease.<sup>100,101</sup>

The imaging goals for most congenital heart diseases include the quantification of blood flow in the great vessels, determination of cardiac chamber volumes and contractility, and assessment of segmental anatomy. Typically, this requires a lengthy MRI scan with over an hour of repeated breath holding under anesthesia, with specialized



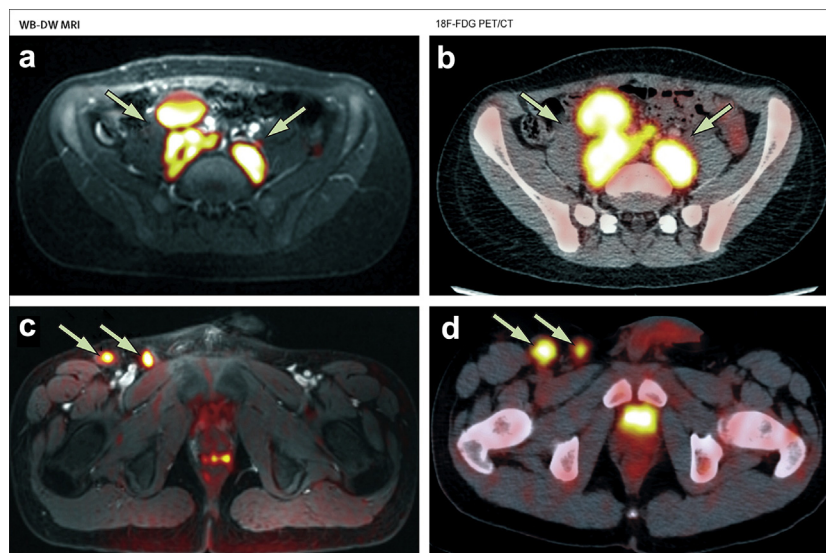


**Figure 15 | Comparison of ionizing radiation-free whole-body diffusion-weighted (WB-DW) magnetic resonance imaging (MRI) scans and 18F-fluorodeoxyglucose positron emission tomography (18F-FDG PET)/computed tomography (CT) scans in the detection of malignant lymphoma.** (a) Axial WB-DW MRI and (b) 18F-FDG PET/CT scans of a 15-year-old patient with stage IIIA Hodgkin lymphoma show positive retroperitoneal lymph nodes (arrows). (c) Axial WB-DW MRI and (d) 18F-FDG PET/CT scans of a 14-year-old patient with class IIB Hodgkin lymphoma show positive right inguinal lymph nodes (arrows). Integrated ferumoxytol-enhanced WB-DW MR images provided equal sensitivities and specificities for cancer staging compared with 18F-FDG-PET/CT.<sup>28</sup> More recent developments combine the advantages of both imaging technologies into 18F-FDG-PET/MRI applications wherein ferumoxytol-enhanced anatomic T1-weighted MR images are merged with 18F-FDG-PET images.<sup>112</sup> On 18F-FDG-PET/MRI scans, ferumoxytol can help to differentiate malignant lymph nodes (18F-FDG positive, no iron uptake) from benign inflammatory nodes (18F-FDG positive with iron uptake), as well as neoplastic bone marrow disease (18F-FDG positive, no iron uptake) from normal hypercellular hematopoietic marrow (18F-FDG positive with iron uptake). From Klenk C, Gawande R, Uslu L, et al. Ionising radiation-free whole-body MRI versus (18F)-fluorodeoxyglucose PET/CT scans for children and young adults with cancer: a prospective, non-randomised, single-centre study. *Lancet Oncol.* 2014;15:275–285,<sup>28</sup> used with permission from *Lancet Oncol.*

print & web 4C/FPO

technologists and physicians on hand to prescribe customized planes for image acquisition. A compelling advantage of ferumoxytol is that it enables volumetric temporally resolved high-resolution imaging without breath holding.<sup>99</sup> Furthermore, a free-breathing volumetric comprehensive MRI yielding flow, function, and anatomic assessment in less than 10 minutes has been achieved.<sup>100</sup> Additionally, ventricular mass may be quantified with this same technique.<sup>101</sup> As a result, no special operator knowledge of cardiac anatomy is required, and the duration of anesthesia and the complexity of the procedure of congenital heart MRI can be greatly reduced. These techniques stand to revolutionize the approach to MRI in children with complex congenital heart diseases.

### Aortic imaging

Aortic imaging can be performed with CT angiography, noncontrast MRI, or gadolinium-enhanced MRA. Blood volume, flow measurements, and morphologic assessments can be made with contrast-enhanced MRA using a combination of time-resolved and steady-state images. Inflammation in the aortic wall can be potentially assessed using *in vivo* macrophage labeling with ferumoxytol, which is not available with gadolinium-enhanced imaging. Inflammation plays a key role in the progression and vulnerability of rupturing atherosclerotic plaques in many arterial

territories. The presence of inflammation can also predict vessel patency.<sup>102,103</sup>

Additionally, because of its long intravascular half-life, ferumoxytol can be used in the detection of aortic endoleaks after endovascular aneurysm repair. A systematic review showed that MRA detected almost twice as many endoleaks as CT angiography.<sup>104</sup> Iron oxide-enhanced MRA (either with ferumoxytol or ferucarbotran) may be advantageous for demonstrating endoleaks.<sup>105,106</sup>

### Visceral arteries and arteriovenous fistulas

Patients with end-organ ischemia in the abdominal vasculature often have diabetes and renal insufficiency. Therefore, ferumoxytol may be a useful agent for assessing renal artery stenosis, pre- and posttransplantation vessel patency, and new venous access. In pre- and postrenal and liver transplantation patients, ferumoxytol has been used to assess vascular integrity.<sup>30,95</sup> The frequent occurrence of venous occlusion in these patients and the requirement to confirm or re-establish venous access make high-resolution venous imaging with ferumoxytol invaluable (Figure 17).<sup>91</sup>

Most studies regarding pre-fistula assessments involve pediatric patients because this group benefits the most from ferumoxytol-enhanced MRA. In a feasibility study using

**Table 3 | Applications, advantages, and disadvantages of ferumoxytol-enhanced magnetic resonance imaging in patients with vascular diseases**

Region	Possibilities	Advantages	Disadvantages
All modalities and general benefits and drawbacks	MRA and MRV Vessel wall visualization First-pass and steady-state images Whole-body imaging	No ionizing radiation Nontoxic contrast agent Noninvasive Multiple planes Long imaging window (blood pool agent) Shows inflammation Highly reproducible	Close physiological monitoring necessary
Carotid and intracerebral arteries	Carotid CE-MRA: - Vascular integrity assessment - Stenosis assessment - Complete plaque morphology evaluation CoW CE-MRA: - CoW evaluation for treatment planning Silent infarction demonstration	Direct visualization of the vessel wall Excellent soft-tissue contrast for plaque analysis More accurate in predicting degree of stenosis than DSA Plaque follow-up, progression monitoring	Close physiological monitoring necessary Not suitable for visualizing calcification
Aorta	Aneurysm Dissection Coarctation Endoleak	Visualization of wall inflammation More sensitive for post-EVAR endoleaks than CTA	Close physiological monitoring necessary
Cardiac	Infective diseases diagnosis Coronary artery visualization Detection and remodeling of myocardial infarct Inflammatory diseases (myocarditis) Congenital heart diseases Chronic heart failure measurements Acute transplant rejection	High-resolution and 3D images of the cardiac chambers and thoracic vessels Global and regional contractile function assessment Blood flow measurements High sensitivity and specificity for acute inflammation Response monitoring for treatment No breath holding Shorter acquisition time	Close physiological monitoring necessary Stents and metallic artifacts
Lower extremities	Lower limb CE-MRA Possibility for blood volume mapping	Postrevascularization increased blood volume can be shown	Difficulty in distinguishing arteries and veins on steady-state images
Visceral arteries	Revascularization follow-up Renal artery evaluation Kidney transplant follow-up Mesenteric ischemia	Beneficial in any stage of renal insufficiency	
Veins	Splenic artery aneurysm Vena cava and iliac vein thrombosis diagnosis and follow-up Agenesis and chronic occlusion Vein mapping prior to dialysis graft placement	The whole abdominopelvic deep venous system is assessable Pulmonary thromboembolism can be visualized (in major vessels) Better sensitivity for thrombus imaging than noncontrast techniques No bolus needed Long imaging window Higher resolution Fewer motion artifacts High SNR	
Pediatric	Congenital heart disease Vascular malformations Kidney diseases and transplantation follow-up	Whole-body imaging is available	Sedation or anesthesia may be needed

CE-MRA, contrast-enhanced MRA; CoW, Circle of Willis; CTA, computed tomography angiography; DSA, digital subtraction angiography; EVAR, endovascular aneurysm repair; MRA, magnetic resonance angiography; MRV, magnetic resonance venography; SNR, signal-to-noise ratio; 3D, 3-dimensional.

ferumoxytol for clinical pediatric cardiovascular imaging, Ruangwattanapaisarn *et al.*<sup>32</sup> evaluated renal transplant or posttransplant complications, vascular shunts, stenosis, aneurysms, and congenital heart disease and obtained excellent image qualities of the hepatic arteries, superior

mesenteric artery, renal arteries, pulmonary arteries, pulmonary veins, valves, and ventricles. Ferumoxytol-enhanced MRA consistently provided superior quality time-of-flight MRA images of patients with arteriovenous fistulas.<sup>96</sup>



print &amp; web 4C/FPO

**Figure 16 | Kawasaki disease.** Multilobed aneurysms (arrows) of the right and left coronary arteries in a 3-year-old patient. Single frame from a multiphase, steady-state imaging with contrast enhancement acquisition.<sup>99</sup> Systemic arteries are colored red. Image provided courtesy of John Paul Finn.

Other applications in vascular imaging (carotid and peripheral artery imaging and MR venography) can be found in the [Supplementary Material 1](#).

## DISCUSSION

In this review, we draw attention to ferumoxytol as a contrast agent for cross-sectional imaging in patients with renal failure and highlight the various clinical indications in which ferumoxytol may not only be an alternative to GBCAs but also may be a specialized contrast agent with unique properties. These include the extended blood pool phase and

uptake into the MPS in the delayed phase, where nanoparticles are metabolized as iron.

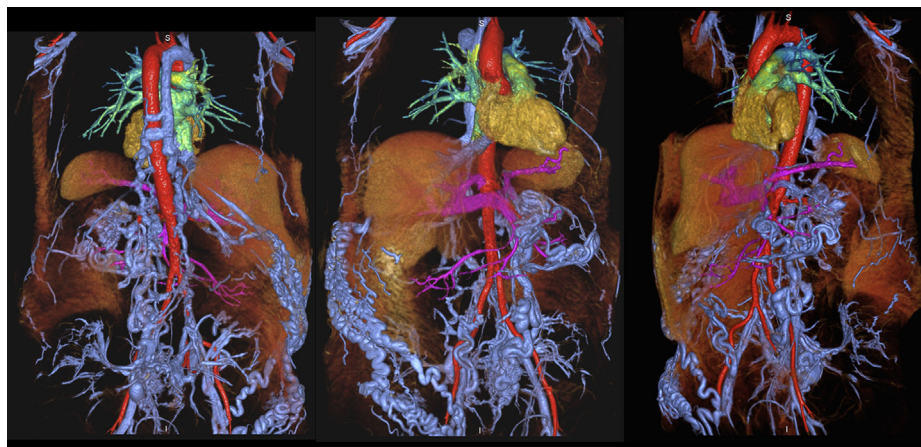
Ferumoxytol has been approved by the FDA for iron replacement in 2009, and it is available for off-label clinical use. A large and growing body of literature has been reviewed in this manuscript showing the potentials of ferumoxytol imaging. Although most available evidence is based on single-center studies, pilot studies, retrospective analyses, and preclinical results, there are new multicenter, multiplatform studies being designed ([clinicaltrials.gov](http://clinicaltrials.gov), NCT02359097). Application for FDA approval for the use of ferumoxytol as an imaging agent is in preparation, which would further ease its widespread use in MRI.

## Limitations

Besides known hypersensitivity or iron metabolic disorders, there is no absolute contraindication for ferumoxytol in MRI, and importantly, it is safe in patients with renal impairment. Vascular visualization improves early after administration, whereas late enhancement visualizes parenchymal-intracellular enhancement, which may require an additional visit, posing a logistical limitation with MRI scheduling. A signal change in the brain may persist from a few days to a week. Uptake in the liver, spleen, and bone marrow may alter MRI signal for months; therefore, radiologists must be aware of any prior history of i.v. iron oxide use. While hypersensitivity reactions occur, the incidence of serious ferumoxytol-related hypersensitivity is very low, and new FDA guidelines aim to further improve patient safety.

## CONCLUSION

In conclusion, there are numerous potential applications of ferumoxytol in MRI throughout the body, including the CNS, various organs outside of the CNS, and cardiovascular system. Whether used in cases wherein GBCAs are contraindicated or for applications that are currently outside the scope of GBCAs, ferumoxytol has shown sufficient promise to warrant



print &amp; web 4C/FPO

**Figure 17 | Volume-rendered reconstruction of an inferior vena cava occlusion in a 58-year-old male with chronic renal failure.** Steady-state, breath-held, high-resolution magnetic resonance angiography with ferumoxytol at 3.0 T. Huge pelvic and abdominal wall collaterals and a dilated azygos vein are clearly visualized Blue, systemic veins; purple, portal vessels; red, systemic arteries. Images provided courtesy of John Paul Finn.



vigorous research into its ultimate clinical role. Radiological modalities that are noninvasive, radiation free, and safe are generally preferred and should be further developed; ferumoxytol MRI may be an important step in this direction.

#### DISCLOSURE

All the authors declared no competing interests.

#### ACKNOWLEDGMENTS

This work was supported in part by the National Institutes of Health grants NS053468 and CA137488-15S1; in part by Federal funds from the National Cancer Institute, under Contract No. HHSN261200800001E; a Veterans Administration Merit Review Grant; and by the Walter S. and Lucienne Driskill Foundation, all to EAN. In addition, JPF was funded by R01 HL127153 IND 129441 (Feraheme as an MRI Contrast Agent for Pediatric Congenital Heart Disease - on clinical trials.gov) and HED by 2R01AR054458, R01 HD081123A, R21CA176519, R21AR066302, and R21CA190196. We kindly thank Emily Youngers for her expert editing of the manuscript.

#### SUPPLEMENTARY MATERIAL

**Supplementary Material 1.** This online supplement was created as complementary material for the review to fully demonstrate the applications of ferumoxytol throughout the body. In this material we discuss the future imaging capabilities of ferumoxytol in the CNS, body, and vasculature and demonstrate all the applications in the form of an atlas with a table of contents and 54 images.

**Supplementary Material 2.** This table was created as supplementary material for the review in order to list the published clinical studies of ferumoxytol by clinical indication.

Supplementary material is linked to the online version of the paper at [www.kidney-international.org](http://www.kidney-international.org).

#### REFERENCES

- Kanda T, Oba H, Toyoda K, et al. Brain gadolinium deposition after administration of gadolinium-based contrast agents. *Jpn J Radiol.* 2016;34:3–9.
- Ramalho J, Semelka RC, AlObaidy M, et al. Signal intensity change on unenhanced T1-weighted images in dentate nucleus following gadobenate dimeglumine in patients with and without previous multiple administrations of gadodiamide. *Eur Radiol.* 2016;26:4080–4088.
- Reeder SB, Gulani V. Gadolinium Deposition in the Brain: Do We Know Enough to Change Practice? *Radiology.* 2016;279:323–336.
- Stojanov D, Aracki-Trenkic A, Benedeto-Stojanov D. Gadolinium deposition within the dentate nucleus and globus pallidus after repeated administrations of gadolinium-based contrast agents-current status. *Neuroradiology.* 2016;58:433–441.
- Kowalczyk M, Banach M, Rysz J. Ferumoxytol: a new era of iron deficiency anemia treatment for patients with chronic kidney disease. *J Nephrol.* 2011;24:717–722.
- Balakrishnan VS, Rao M, Kausz AT, et al. Physicochemical properties of ferumoxytol, a new intravenous iron preparation. *Eur J Clin Invest.* 2009;39:489–496.
- Hetzel D, Strauss W, Bernard K, et al. A phase III, randomized, open-label trial of ferumoxytol compared with iron sucrose for the treatment of iron deficiency anemia in patients with a history of unsatisfactory oral iron therapy. *Am J Hematol.* 2014;89:646–650.
- Macdougall IC, Strauss WE, McLaughlin J, et al. A randomized comparison of ferumoxytol and iron sucrose for treating iron deficiency anemia in patients with CKD. *Clin J Am Soc Nephrol.* 2014;9:705–712.
- Vadhan-Raj S, Ford DC, Dahl NV, et al. Safety and efficacy of ferumoxytol for the episodic treatment of iron deficiency anemia in patients with a history of unsatisfactory oral iron therapy: Results of a phase III, open-label, 6-month extension study. *Am J Hematol.* 2016;91:E3–E5.
- Gahramanov S, Muldoon LL, Varallyay CG, et al. Pseudoprogression of glioblastoma after chemo- and radiation therapy: diagnosis by using dynamic susceptibility-weighted contrast-enhanced perfusion MR imaging with ferumoxytol versus gadoteridol and correlation with survival. *Radiology.* 2013;266:842–852.
- US Food and Drug Administration. FDA Drug Safety Communication: FDA strengthens warnings and changes prescribing instructions to decrease the risk of serious allergic reactions with anemia drug Feraheme (ferumoxytol). 2015.
- Christen T, Ni W, Qiu D, et al. High-resolution cerebral blood volume imaging in humans using the blood pool contrast agent ferumoxytol. *Magn Reson Med.* 2013;70:705–710.
- Varallyay CG, Nesbit E, Fu R, et al. High-resolution steady-state cerebral blood volume maps in patients with central nervous system neoplasms using ferumoxytol, a superparamagnetic iron oxide nanoparticle. *J Cereb Blood Flow Metab.* 2013;33:780–786.
- Finn JP, Nguyen KL, Han F, et al. Cardiovascular MRI with ferumoxytol. *Clin Radiol.* 2016;71:796–806.
- Neuwelt EA, Várallyay CG, Manninger S, et al. The potential of ferumoxytol nanoparticle magnetic resonance imaging, perfusion, and angiography in central nervous system malignancy: a pilot study. *Neurosurgery.* 2007;60:601–611; discussion 11–12.
- Harisinghani M, Ross RW, Guimaraes AR, Weissleder R. Utility of a new bolus-injectable nanoparticle for clinical cancer staging. *Neoplasia.* 2007;9:1160–1165.
- Hedgire S, Mino-Kenudson M, Elmi A, et al. Enhanced primary tumor delineation in pancreatic adenocarcinoma using ultrasmall superparamagnetic iron oxide nanoparticle-ferumoxytol: an initial experience with histopathologic correlation. *Int J Nanomedicine.* 2014;9:1891–1896.
- Daldrup-Link HE, Golovko D, Ruffell B, et al. MRI of tumor-associated macrophages with clinically applicable iron oxide nanoparticles. *Clin Cancer Res.* 2011;17:5695–5704.
- McConnell HL, Schwartz DL, Richardson BE, et al. Ferumoxytol nanoparticle uptake in brain during acute neuroinflammation is cell-specific. *Nanomedicine.* 2016;12:1535–1542.
- Muehe AM, Feng D, von Eyben R, et al. Safety report of ferumoxytol for magnetic resonance imaging in children and young adults. *Invest Radiol.* 2016;51:221–227.
- Provenzano R, Schiller B, Rao M, et al. Ferumoxytol as an intravenous iron replacement therapy in hemodialysis patients. *Clin J Am Soc Nephrol.* 2009;4:386–393.
- Singh A, Patel T, Hertel J, et al. Safety of ferumoxytol in patients with anemia and CKD. *Am J Kidney Dis.* 2008;52:907–915.
- Spinowitz BS, Kausz AT, Baptista J, et al. Ferumoxytol for treating iron deficiency anemia in CKD. *J Am Soc Nephrol.* 2008;19:1599–1605.
- Schiller B, Bhat P, Sharma A. Safety and effectiveness of ferumoxytol in hemodialysis patients at 3 dialysis chains in the United States over a 12-month period. *Clin Ther.* 2014;36:70–83.
- Bashir MR, Mody R, Neville A, et al. Retrospective assessment of the utility of an iron-based agent for contrast-enhanced magnetic resonance venography in patients with endstage renal diseases. *J Magn Reson Imaging.* 2014;40:113–118.
- D'Arceuil H, Coimbra A, Triano P, et al. Ferumoxytol enhanced resting state fMRI and relative cerebral blood volume mapping in normal human brain. *NeuroImage.* 2013;83:200–209.
- Hasan DM, Amans M, Tihan T, et al. Ferumoxytol-enhanced MRI to Image Inflammation within Human Brain Arteriovenous Malformations: A Pilot Investigation. *Transl Stroke Res.* 2012;3(Suppl 1):166–173.
- Klenk C, Gawande R, Uslu L, et al. Ionising radiation-free whole-body MRI versus (18)F-fluorodeoxyglucose PET/CT scans for children and young adults with cancer: a prospective, non-randomised, single-centre study. *Lancet Oncol.* 2014;15:275–285.
- Li W, Tutton S, Vu AT, et al. First-pass contrast-enhanced magnetic resonance angiography in humans using ferumoxytol, a novel ultrasmall superparamagnetic iron oxide (USPIO)-based blood pool agent. *J Magn Reson Imaging.* 2005;21:46–52.
- Nayak AB, Luhar A, Hanudel M, et al. High-resolution, whole-body vascular imaging with ferumoxytol as an alternative to gadolinium agents in a pediatric chronic kidney disease cohort. *Pediatr Nephrol.* 2015;30:515–521.
- Ning P, Zucker EJ, Wong P, Vasawala SS. Hemodynamic safety and efficacy of ferumoxytol as an intravenous contrast agents in pediatric patients and young adults. *Magn Reson Imaging.* 2016;34:152–158.

32. Ruangwattanapaisarn N, Hsiao A, Vasanaawala SS. Ferumoxytol as an off-label contrast agent in body 3T MR angiography: a pilot study in children. *Pediatr Radiol*. 2015;45:831–839.
33. Thompson EM, Guillaume DJ, Dosa E, et al. Dual contrast perfusion MRI in a single imaging session for assessment of pediatric brain tumors. *J Neurooncol*. 2012;109:105–114.
34. Walker JP, Nosova E, Sigovan M, et al. Ferumoxytol-enhanced magnetic resonance angiography is a feasible method for the clinical evaluation of lower extremity arterial disease. *Ann Vasc Surg*. 2015;29:63–68.
35. Vasanaawala SS, Nguyen KL, Hope MD, et al. Safety and technique of ferumoxytol administration for MRI. *Magn Reson Med*. 2016;75:2107–2111.
36. Hamilton BE, Nesbit GM, Dosa E, et al. Comparative analysis of ferumoxytol and gadoteridol enhancement using T1- and T2-weighted MRI in neuroimaging. *AJR Am J Roentgenol*. 2011;197:981–988.
37. Dósa E, Guillaume DJ, Haluska M, et al. Magnetic resonance imaging of intracranial tumors: intra-patient comparison of gadoteridol and ferumoxytol. *Neuro Oncol*. 2011;13:251–260.
38. Hamilton BE, Ambady P, Nesbit G, et al. Ferumoxytol enhanced MRI detection of intracranial metastatic disease [abstract no. O-90]. Presented at: American Society of Neuroradiology 54<sup>th</sup> Annual Meeting. May 23–26, 2016; Washington, DC.
39. Aghighi M, Golovko D, Ansari C, et al. Imaging tumor necrosis with ferumoxytol. *PLoS One*. 2015;10:e0142665.
40. Dósa E, Tuladhar S, Muldoon LL, et al. MRI using ferumoxytol improves the visualization of central nervous system vascular malformations. *Stroke*. 2011;42:1581–1588.
41. Neuwelt EA, Hamilton BE, Varallyay CG, et al. Ultrasmall superparamagnetic iron oxides (USPIOs): a future alternative magnetic resonance (MR) contrast agent for patients at risk for nephrogenic systemic fibrosis (NSF)? *Kidney Int*. 2009;75:465–474.
42. Hamilton BE, Woltjer RL, Prola-Netto J, et al. Ferumoxytol-enhanced MRI differentiation of meningioma from dural metastases: a pilot study with immunohistochemical observations. *J Neurooncol*. 2016;129:301–309.
43. Abdoli M, Freedman MS. Neuro-oncology dilemma: Tumour or tumefactive demyelinating lesion. *Mult Scler Relat Disord*. 2015;4:555–566.
44. Farrell BT, Hamilton BE, Dosa E, et al. Using iron oxide nanoparticles to diagnose CNS inflammatory diseases and PCNSL. *Neurology*. 2013;81:256–263.
45. Law M, Yang S, Wang H, et al. Glioma grading: sensitivity, specificity, and predictive values of perfusion MR imaging and proton MR spectroscopic imaging compared with conventional MR imaging. *AJNR Am J Neuroradiol*. 2003;24:1989–1998.
46. Danchaivijitr N, Waldman AD, Tozer DJ, et al. Low-grade gliomas: do changes in rCBV measurements at longitudinal perfusion-weighted MR imaging predict malignant transformation? *Radiology*. 2008;247:170–178.
47. Brandsma D, Stalpers L, Taal W, et al. Clinical features, mechanisms, and management of pseudoprogression in malignant gliomas. *Lancet Oncol*. 2008;9:453–461.
48. Nasser M, Gahramanov S, Netto JP, et al. Evaluation of pseudoprogression in patients with glioblastoma multiforme using dynamic magnetic resonance imaging with ferumoxytol calls RANO criteria into question. *Neuro Oncol*. 2014;16:1146–1154.
49. Varallyay CG, Muldoon LL, Gahramanov S, et al. Dynamic MRI using iron oxide nanoparticles to assess early vascular effects of antiangiogenic versus corticosteroid treatment in a glioma model. *J Cereb Blood Flow Metab*. 2009;29:853–860.
50. Cohen JV, Alomari AK, Vortmeyer AO, et al. Melanoma Brain Metastasis Pseudoprogression after Pembrolizumab Treatment. *Cancer Immunol Res*. 2016;4:179–182.
51. Hodi FS, Hwu WJ, Kefford R, et al. Evaluation of Immune-Related Response Criteria and RECIST v1.1 in Patients With Advanced Melanoma Treated With Pembrolizumab. *J Clin Oncol*. 2016;34:1510–1517.
52. Okada H, Weller M, Huang R, et al. Immunotherapy response assessment in neuro-oncology: a report of the RANO working group. *Lancet Oncol*. 2015;16:e534–e542.
53. Gahramanov S, Varallyay C, Tyson RM, et al. Diagnosis of pseudoprogression using MRI perfusion in patients with glioblastoma multiforme may predict improved survival. *CNS Oncol*. 2014;3:389–400.
54. Vellinga MM, Oude Engberink RD, Seewann A, et al. Pluriformity of inflammation in multiple sclerosis shown by ultra-small iron oxide particle enhancement. *Brain*. 2008;131:800–807.
55. Tagge I, Kohama S, Pollaro J, et al. Vascular expansion and blood-brain-barrier permeability: a comparative volumetric study in acute Japanese macaque encephalomyelitis [abstract nr 4331]. Presented at: International Society for Magnetic Resonance in Medicine (ISMRM) 24th Annual Meeting. May 30–June 5, 2015; Toronto, Ontario, Canada.
56. Axthelm MK, Bourdette DN, Marracci GH, et al. Japanese macaque encephalomyelitis: a spontaneous multiple sclerosis-like disease in a nonhuman primate. *Ann Neurol*. 2011;70:362–373.
57. Bashir MR, Bhatti L, Marin D, Nelson RC. Emerging applications for ferumoxytol as a contrast agent in MRI. *J Magn Reson Imaging*. 2015;41:884–898.
58. Milot L, Haider M, Foster L, et al. Gadofosveset trisodium in the investigation of focal liver lesions in noncirrhotic liver: Early experience. *J Magn Reson Imaging*. 2012;36(3):738–742.
59. Liu T, Choi H, Zhou R, Chen IW. Quantitative evaluation of the reticuloendothelial system function with dynamic MRI. *PLoS One*. 2014;9:e103576.
60. Olive K, Jacobetz M, Davidson C, et al. Inhibition of Hedgehog signaling enhances delivery of chemotherapy in a mouse model of pancreatic cancer. *Science*. 2009;324:1457–1461.
61. Boxerman J, Hamberg L, Rosen B, Weisskoff R. MR contrast due to intravascular magnetic susceptibility perturbations. *Magn Reson Med*. 1995;34:555–566.
62. Bremer C, Mustafa M, Bogdanov A Jr., et al. Steady-state blood volume measurements in Experimental tumors with different angiogenic burdens - a study in mice. *Radiology*. 2003;226:214–220.
63. Dennie J, Mandeville J, Boxerman J, et al. NMR imaging of changes in vascular morphology due to tumor angiogenesis. *Magn Reson Med*. 1998;40:793–799.
64. Guimaraes A, Rakhlin E, Weissleder R, Thayer S. Magnetic resonance imaging monitors physiological changes with antihedgehog therapy in pancreatic adenocarcinoma xenograft model. *Pancreas*. 2008;37:440–444.
65. Farrar CT, Kamoun WS, Ley CD, et al. In Vivo validation of MRI vessel caliber index measurement methods with intravital optical microscopy in a u87 mouse brain tumor. *Neuro Oncol*. 2010;12:341–350.
66. Emblem K, Farrar C, Gerstner E, et al. Vessel caliber—a potential MRI biomarker of tumour response in clinical trials. *Nat Rev Clin Oncol*. 2014;11:566–584.
67. Flexman J, Yung A, Yapp D, et al. Assessment of vessel size by MRI in orthotopic model of human pancreatic cancer. *Conf Proc IEEE Eng Med Biol Soc*. 2008;2008:851–854.
68. Guimaraes A, Ross R, Figueiredo J, et al. MRI with magnetic nanoparticles monitors downstream anti-angiogenic effects of mTOR inhibition. *Mol Imaging Biol*. 2011;13:314–320.
69. Jensen J, Chandra R. MR imaging of microvasculature. *Magn Reson Med*. 2000;44:224–230.
70. Kiselev V, Strecker R, Ziyeh S, et al. Vessel size imaging in humans. *Magn Reson Med*. 2005;53:553–563.
71. Lemasson B, Valable S, Farion R, et al. In vivo imaging of vessel diameter, size, and density: a comparative study between MRI and histology. *Magn Reson Med*. 2013;69:18–26.
72. Tropes I, Grimault S, Vaeth A, et al. Vessel size imaging. *Magn Reson Med*. 2001;45:397–408.
73. Weissleder R, Elizaondo G, Wittenberg J, et al. Ultrasmall superparamagnetic iron oxide: characterization of a new class of contrast agents for MR imaging. *Radiology*. 1990;175:489–493.
74. Gaglia J, Guimaraes A, Harisinghani M, et al. Noninvasive imaging of pancreatic islet inflammation in type 1A diabetes patients. *J Clin Invest*. 2011;121:442–445.
75. Gaglia J, Harisinghani M, Aganj I, et al. Noninvasive mapping of pancreatic inflammation in recent-onset type-1 diabetes patients. *Proc Natl Acad Sci U S A*. 2015;112:2139–2144.
76. Ganeshalingam S, Koh DM. Nodal staging. *Cancer Imaging*. 2009;9:104–111.
77. Barentsz J. MR imaging of pelvic lymph nodes. *Cancer Imaging*. 2003;3:130–134.
78. Harisinghani MG, Saini S, Slater GJ, et al. MR imaging of pelvic lymph nodes in primary pelvic carcinoma with ultrasmall superparamagnetic iron oxide (Combidex): preliminary observations. *J Magn Reson Imaging*. 1997;7:161–163.

79. Anzai Y, Piccoli CW, Outwater EK, et al. Evaluation of neck and body metastases to nodes with ferumoxtran 10-enhanced MR imaging: phase III safety and efficacy study. *Radiology*. 2003;228:777–788.
80. Wolf JS Jr., Cher M, Dall'era M, et al. The use and accuracy of cross-sectional imaging and fine needle aspiration cytology for detection of pelvic lymph node metastases before radical prostatectomy. *J Urol*. 1995;153:993–999.
81. Turkbey B, Agarwal HK, Shih J, et al. A phase I dosing study of ferumoxytol for MR lymphography at 3 T in patients with prostate cancer. *AJR Am J Roentgenol*. 2015;205:64–69.
82. Sankineni S, Smedley J, Bernardo M, et al. Ferumoxytol as an intraprostatic MR contrast agent for lymph node mapping of the prostate: a feasibility study in non-human primates. *Acta Radiol*. 2015;57:1396–1401.
83. Hasan D, Chalouhi N, Jabbour P, et al. Early change in ferumoxytol-enhanced magnetic resonance imaging signal suggests unstable human cerebral aneurysm: a pilot study. *Stroke*. 2012;43:3258–3265.
84. Wagner S, Schnorr J, Ludwig A, et al. Contrast-enhanced MR imaging of atherosclerosis using citrate-coated superparamagnetic iron oxide nanoparticles: calcifying microvesicles as imaging target for plaque characterization. *Int J Nanomedicine*. 2013;8:767–779.
85. Budjan J, Neudecker S, Schock-Kusch D, et al. Can Ferumoxytol be Used as a Contrast Agent to Differentiate Between Acute and Chronic Inflammatory Kidney Disease?: Feasibility Study in a Rat Model. *Invest Radiol*. 2016;51:100–105.
86. Rogers JL, Tarrant T, Kim JS. Nanoparticle-based diagnostic imaging of inflammation in rheumatic disease. *Curr Rheumatology Rev*. 2014;10:3–10.
87. Simon GH, von Vopelius-Feldt J, Fu Y, et al. Ultrasmall superparamagnetic iron oxide-enhanced magnetic resonance imaging of antigen-induced arthritis: a comparative study between SHU 555 C, ferumoxtran-10, and ferumoxytol. *Invest Radiol*. 2006;41:45–51.
88. Neuwelt A, Langsjoen J, Byrd T, et al. Ferumoxytol negatively enhances T2-weighted MRI of pedal osteomyelitis in vivo. *J Magn Reson Imaging*. 2017;45:1241–1245.
89. Neuwelt A, Sidhu N, Hu CA, et al. Iron-based superparamagnetic nanoparticle contrast agents for MRI of infection and inflammation. *AJR Am J Roentgenol*. 2015;204:W302–W313.
90. Moy MP, Sauk J, Gee MS. The role of MR enterography in assessing Crohn's disease activity and treatment response. *Gastroenterol Res Pract*. 2016;2016:8168695.
91. Luhar A, Khan S, Finn JP, et al. Contrast-enhanced magnetic resonance venography in pediatric patients with chronic kidney disease: initial experience with ferumoxytol. *Pediatr Radiol*. 2016;46:1332–1340.
92. Uslu L, Donig J, Link M, et al. Value of 18F-FDG PET and PET/CT for evaluation of pediatric malignancies. *J Nucl Med*. 2015;56:274–286.
93. Marso SP, Hiatt WR. Peripheral arterial disease in patients with diabetes. *J Am Coll Cardiol*. 2006;47:921–929.
94. Nathan DP, Tang GL. The impact of chronic renal insufficiency on vascular surgery patient outcomes. *Semin Vasc Surg*. 2014;27:162–169.
95. Bashir MR, Jaffe TA, Brennan TV, et al. Renal transplant imaging using magnetic resonance angiography with a nonnephrotoxic contrast agent. *Transplantation*. 2013;96:91–96.
96. Sigovan M, Gasper W, Alley HF, et al. USPIO-enhanced MR angiography of arteriovenous fistulas in patients with renal failure. *Radiology*. 2012;265:584–590.
97. Alam SR, Shah AS, Richards J, et al. Ultrasmall superparamagnetic particles of iron oxide in patients with acute myocardial infarction: early clinical experience. *Circ Cardiovasc Imaging*. 2012;5:559–565.
98. Yilmaz A, Dengler MA, van der Kuip H, et al. Imaging of myocardial infarction using ultrasmall superparamagnetic iron oxide nanoparticles: a human study using a multi-parametric cardiovascular magnetic resonance imaging approach. *Eur Heart J*. 2013;34:462–475.
99. Han F, Rapacchi S, Khan S, et al. Four-dimensional, multiphase, steady-state imaging with contrast enhancement (MUSIC) in the heart: a feasibility study in children. *Magnetic Reson Med*. 2015;74:1042–1049.
100. Cheng JY, Hanneman K, Zhang T, et al. Comprehensive motion-compensated highly accelerated 4D flow MRI with ferumoxytol enhancement for pediatric congenital heart disease. *J Magn Reson Imaging*. 2016;43:1355–1368.
101. Hanneman K, Kino A, Cheng JY, et al. Assessment of the precision and reproducibility of ventricular volume, function, and mass measurements with ferumoxytol-enhanced 4D flow MRI. *J Magn Reson Imaging*. 2016;44:383–392.
102. DeSart K, O'Malley K, Schmit B, et al. Systemic inflammation as a predictor of clinical outcomes after lower extremity angioplasty/stenting. *J Vasc Surg*. 2016;64:766–778.
103. Okura H, Takagi T, Yoshida K. Therapies targeting inflammation after stent implantation. *Curr Vasc Pharmacol*. 2013;11:399–406.
104. Habets J, Zandvoort HJ, Reitsma JB, Bartels LW, Moll FL, Leiner T, et al. Magnetic resonance imaging is more sensitive than computed tomography angiography for the detection of endoleaks after endovascular abdominal aortic aneurysm repair: a systematic review. *Eur J Vasc Endovasc Surg*. 2013;45:340–350.
105. Ersoy H, Jacobs P, Kent CK, Prince MR. Blood pool MR angiography of aortic stent-graft endoleak. *AJR Am J Roentgenol*. 2004;182:1181–1186.
106. Ichihashi S, Marugami N, Tanaka T, et al. Preliminary experience with superparamagnetic iron oxide-enhanced dynamic magnetic resonance imaging and comparison with contrast-enhanced computed tomography in endoleak detection after endovascular aneurysm repair. *J Vasc Surg*. 2013;58:66–72.
107. Corot C, Robert P, Idee JM, Port M. Recent advances in iron oxide nanocrystal technology for medical imaging. *Adv Drug Deliv Rev*. 2006;58:1471–1504.
108. Blockley NP, Jiang L, Gardener AG, et al. Field strength dependence of R1 and R2\* relaxivities of human whole blood to ProHance, Vasovist, and deoxyhemoglobin. *Magn Reson Med*. 2008;60:1313–1320.
109. Landry R, Jacobs PM, Davis R, et al. Pharmacokinetic study of ferumoxytol: a new iron replacement therapy in normal subjects and hemodialysis patients. *Am J Nephrol*. 2005;25:400–410.
110. Neuwelt EA, Varallyay CG, Manninger S, et al. The potential of ferumoxytol nanoparticle magnetic resonance imaging, perfusion, and angiography in central nervous system malignancy: a pilot study. *Neurosurgery*. 2007;60:601–611; discussion 11–12.
111. Akeson P, Nordstrom CH, Holtas S. Time-dependency in brain lesion enhancement with gadodiamide injection. *Acta Radiol*. 1997;38:19–24.
112. Aghighi M, Pisani LJ, Sun Z, et al. Speeding up PET/MR for cancer staging of children and young adults. *Eur Radiol*. 2016;26:4239–4248.